JB Journals.ASM.org

Articles of Significant Interest Selected from This Issue by the Editors

Defining the Function of Flagellar Protein FliL Offers Clues on How Cells Sense a Surface

Studies with several bacteria species have implicated FliL, a flagellar motor-associated protein, as critical to swarming motility and, in *Proteus mirabilis*, mechanosensing of a surface prior to biofilm formation. Lee and Belas (p. 159–173) have constructed a near-total deletion of *P. mirabilis fliL*. In contrast with other *fliL* defects, cells with a deletion of *fliL* possess temperature-dependent swarming and become more responsive to low-viscosity surfaces. A Δ*fliL* strain of *Escherichia coli* phenocopies the *P. mirabilis* Δ*fliL* strain in being Swr^+ with an alteration in temperature-dependent motility. These results suggest a role for FliL in modulating motor energetics during biofilm formation.

Structural Insight to the Mechanism of Rot-Mediated Regulation in *Staphylococcus aureus*

Repressor of toxin (Rot) is a key regulator of virulence genes in *Staphylococcus aureus*. Killikelly et al. (p. 188–200) determined a crystal structure of Rot to 1.7-Å resolution. The structure facilitated the identification of residues involved in DNA binding and function. For instance, R91, in the wing loop of the DNA binding domain, and L54/K55, adjacent to the wing, were found to be critical for Rot activity. Interestingly, several additional residues were identified as critical for promoter-specific effects, suggesting that Rot differentially regulates target promoters. Altogether, this study provides a molecular blueprint on how Rot controls *S. aureus* virulence.

Watching Bacteria Getting Osmotically Shocked and Measuring How the Shock Rate Affects Survival

Bialecka-Fornal et al. (p. 231–237) have developed a new assay to evaluate mechanosensitive channels in bacteria. Using a combination of microscopy and microfluidics, they are able to directly observe how bacteria respond to osmotic shocks at various shock rates. They find that how much a given channel type protects against shock depends strongly on how fast the osmolarity is changed. After the shock, they observed cells undergo different death mechanisms, other than just popping like a balloon. These findings require a revision of the current paradigm of how shocked cells lyse after shock.

doi:10.1128/JB.02473-14

JB
Journals.ASM.org

Loss of FliL Alters *Proteus mirabilis* Surface Sensing and Temperature-Dependent Swarming

Yi-Ying Lee, Robert Belas

Department of Marine Biotechnology, University of Maryland Baltimore County, and Institute of Marine and Environmental Technology, Baltimore, Maryland, USA

Proteus mirabilis **is a dimorphic motile bacterium well known for its flagellum-dependent swarming motility over surfaces. In liquid, *P. mirabilis* cells are 1.5- to 2.0-μm swimmer cells with 4 to 6 flagella. When *P. mirabilis* encounters a solid surface, where flagellar rotation is limited, swimmer cells differentiate into elongated (10- to 80-μm), highly flagellated swarmer cells. In order for *P. mirabilis* to swarm, it first needs to detect a surface. The ubiquitous but functionally enigmatic flagellar basal body protein FliL is involved in *P. mirabilis* surface sensing. Previous studies have suggested that FliL is essential for swarming through its involvement in viscosity-dependent monitoring of flagellar rotation. In this study, we constructed and characterized Δ*fliL* mutants of *P. mirabilis* and *Escherichia coli*. Unexpectedly and unlike other *fliL* mutants, both *P. mirabilis* and *E. coli* Δ*fliL* cells swarm (Swr$^+$). Further analysis revealed that *P. mirabilis* Δ*fliL* cells also exhibit an alteration in their ability to sense a surface: e.g., Δ*fliL P. mirabilis* cells swarm precociously over surfaces with low viscosity that normally impede wild-type swarming. Precocious swarming is due to an increase in the number of elongated swarmer cells in the population. Loss of *fliL* also results in an inhibition of swarming at <30°C. *E. coli* Δ*fliL* cells also exhibit temperature-sensitive swarming. These results suggest an involvement of FliL in the energetics and function of the flagellar motor.**

Most bacteria are able to live a planktonic free-living lifestyle or in a surface-attached microbial community called a "biofilm." The interchange between the motile and the sessile phases, referred to as the "swim-or-stick" switch, is not merely stochastic. Rather, the lifestyle change occurs in response to cues that a cell senses as it nears a surface (1). These surface signals are required and initiate biofilm formation (1). A fundamental question underlying the transition in lifestyle from motile to sessile phases is how does a bacterium sense a surface?

Studies of many different bacterial species support the idea that surface sensing often involves the bacterial flagellum (2), which also facilitates movement toward and attachment to a surface. However, it is generally agreed that motility and biofilm formation are mutually exclusive. Moreover, flagella are used not only for swimming in liquid but also for swarming over a solid surface. Many bacterial species swarm, and often, as in *Proteus mirabilis*, require a surface-induced differentiated cell type, called a swarmer cell, that is elongated and hyperflagellated (3).

P. mirabilis is a Gram-negative gammaproteobacterium belonging to the *Enterobacteriaceae* family. It is an opportunistic pathogen capable of causing urinary tract infections (UTI) (4–6). *P. mirabilis* is dimorphic and produces short vegetative swimmer cells (1.5 to 2.0 μm in length) with a single nucleoid and 4 to 10 peritrichous flagella when cultured in nutrient broth. Conversely, when cultured on nutrient agar or in viscous environments, *P. mirabilis* swimmer cells differentiate into nonseptated, elongated (10 to 80 μm in length) swarmer cells with multiple nucleoids and numerous flagella (4, 7). *P. mirabilis* cells monitor the rotation of their flagella to recognize and sense surface contact. When a swimmer cell encounters a solid surface or viscous environment, inhibition of flagellar rotation triggers differentiation into a swarmer cell (8). Furthermore, on a surface, swarmer cells align with one another to perform a multicellular coordinative movement, known as "swarming" (4). *P. mirabilis* swarmer cell differentiation is correlated with elevated expression of several virulence factors that aid in the invasion of uroepithelial cells in human urinary tracts (4, 9).

P. mirabilis swarming may be divided into four stages: (i) surface-induced swarmer cell differentiation, (ii) a lag period of ca. 3.25 h prior to swarming migration, (iii) active swarming migration, and (iv) a consolidation phase, during which swarmer cells stop moving and dedifferentiate into swimmer-like cells. The four stages are cyclic and give rise to the distinctive bull's-eye colony pattern when *P. mirabilis* is grown on nutrient agar (10, 11).

Both swimming motility and swarming motility require functional flagella. The bacterial flagellum is a complex, extracellular filamentous structure that consists of three parts: a rotary basal body associated with the membrane, a hook junction, and an extended helical filament (12). The hook-basal body (HBB) complex is a rotary motor powered by proton motive force (PMF), which is generated by proton translocation through the stator complex, encoded by *motA* and *motB* (12). Genes involved in flagellum biosynthesis are clustered in several operons that make up the flagellar regulon. In *P. mirabilis* and other enteric bacteria, expression of the flagellar regulon is governed by a three-tiered hierarchical control allowing the coordinate expression of flagellar genes and flagellum biosynthesis (13). The *flhDC* operon (ex-

Received 21 August 2014 **Accepted** 13 October 2014

Accepted manuscript posted online 20 October 2014

Citation Lee Y-Y, Belas R. 2015. Loss of FliL alters *Proteus mirabilis* surface sensing and temperature-dependent swarming. J Bacteriol 197:159–173. doi:10.1128/JB.02235-14.

Editor: J. P. Armitage

Address correspondence to Robert Belas, belas@umbc.edu.

Supplemental material for this article may be found at http://dx.doi.org/10.1128/JB.02235-14.

doi:10.1128/JB.02235-14

pressed from a class 1 promoter) encodes the flagellar master transcriptional regulatory protein complex, $FlhD_4C_2$. $FlhD_4C_2$ activates expression of class 2 promoters that transcribe genes such as *fliA*, encoding the flagellum-specific σ^{28} factor, *flgM*, encoding FlgM, an anti-σ^{28} factor, and genes encoding proteins comprising the HBB complex and the type III flagellar secretion apparatus. FliA is required for transcription of class 3 promoters, whose genes include those required for the production of the flagellar filament, the stator complex, and those involved in chemotactic behavior (14–16).

$FlhD_4C_2$ plays a central role in *P. mirabilis* swarmer cell differentiation (17). When *P. mirabilis* swimmer cells differentiate into swarmer cells, *flhDC* transcription increases, and genes in the flagellar regulon are upregulated (16, 18, 19). Many regulatory and environmental factors control the expression and activity of *flhDC* and swarming. For example, studies in *Escherichia coli* have shown that transcription of the *flhDC* operon is negatively regulated by the RcsCDB phosphorelay system (20), composed of the sensor kinase, RcsC, which passes a phosphoryl group to its cognate response regulator, RcsB, via RcsD, a phosphotransferase. Phosphorylated RcsB negatively regulates *flhDC* (21). Mutations in the components of *P. mirabilis* Rcs system result in increased expression of *flhDC* and precocious swarming: e.g., the swarming lag phase is shortened and swarming migration initiates earlier than in wild-type cells (22–24). *P. mirabilis* contains the four genes *umoA* to *-D*, two of which are known to interact with the Rcs system to increase expression of *flhDC*. These *umo* (i.e., upregulator of the master operon) genes were first identified as suppressors of the swarming defect in an *flgN* mutant, which is defective in a flagellar chaperone (25). The Umo proteins are predicted to be located in the cell envelope (25). *umoA*, encoding a putative outer membrane protein, contains both σ^{70}-dependent and σ^{28}-dependent (flagellar class 3) promoters (25), hinting that *umoA* may be a novel member of the flagellar regulon. Morgenstein and Rather have suggested that UmoB and UmoD are in a pathway that activates the Rcs phosphorelay system (26). How the Umo proteins function to increase *flhDC* expression is unclear.

Most flagellar genes have well-understood functions in bacterial motility, but *fliL* is an exception, and the role of FliL in flagellar structure and energetics remains, at best, obscure. In many species, *fliL* is the first gene of a class 2 operon, *fliLMNOPQR*, which is controlled by both $FlhD_4C_2$ and FliA. This operon encodes C-ring proteins (FliMN), components of the rotor of the flagellar motor and situated at the cytoplasmic face of the inner membrane, and those (FliOPQR) involved in the export apparatus. FliL is a small transmembrane protein (ca. 18 kDa in most species) located adjacent to the basal body and in close proximity to MotAB (27–29). FliL has a single transmembrane (TM) domain (residues 12 to 38 of 160 residues in *P. mirabilis*) near its N terminus, such that the N terminus of FliL is in the cytoplasm, while the rest of the protein is in the periplasm.

Among bacterial species, the phenotype of *fliL* cells is diverse. In alphaproteobacteria, such as *Rhodobacter sphaeroides*, *Silicibacter* sp. strain TM1040, and *Caulobacter crescentus*, disruption of *fliL* results in nonmotile cells (30–32), which is also true for *fliL* defects in the spirochete *Borrelia burgdorferi* (29). In gammaproteobacteria, such as *Escherichia coli*, *Salmonella enterica* serovar Typhimurium ("*S. enterica*" herein), and *P. mirabilis*, *fliL* mutations result in a minor decrease in swimming but severely affect swarming (27, 33, 34).

Our laboratory is interested in understanding the mechanism used by *P. mirabilis* to detect a surface and subsequently produce a swarmer cell. Transposon mutagenesis has proven to be valuable in identifying genes important for swarming and swarmer cell differentiation of *P. mirabilis* (35). Due to the polar nature of the mutation, insertion of a transposon in a flagellar gene often results in nonswarming (Swr^-) cells that do not differentiate on surfaces. However, a small class of Tn*5* insertion mutants, notably those with mutation in *fliL* (e.g., strain BB2204), are different because these *fliL* defects produce elongated swarmer-like cells (Elo^+ [pseudoswarmer cells]) in noninducing liquid environments (8). BB2204 pseudoswarmer cells phenocopy most of the hallmarks of swarmer cells, such as cell elongation and polyploidy, but they do not produce flagella due to polar effects on *fliMNOPQR* (8, 34). We use the pseudoswarmer Elo^+ phenotype as a proxy indicating that the surface-sensing mechanism has detected and responded to a surface. As such, the production of a pseudoswarmer cell under normally noninducing conditions indicates that the surface-sensing mechanism has malfunctioned and inappropriately signaled that the cell is on a surface when it is not.

To alleviate the unwanted polarity associated with transposon insertions in *fliL* (and the resulting loss of flagellar synthesis), in a previous report (18), we selected for a spontaneous *fliL* Swr^+ mutant (YL1001) that had a partial excision of Tn*5* from its BB2204 parent. This mutation altered the last 14 amino acids of FliL and restored transcription of *fliMNOPQR*, flagellum synthesis, and swarming, while retaining the Elo^+ phenotype. This result demonstrates that the C terminus of FliL is involved in surface sensing (8, 18, 34). More recently, we constructed a nonpolar *fliL*-null mutant (*fliL*::*kan*-nt 30 [YL1003]) that resulted in the production of a severely truncated FliL protein. This *fliL* mutant is Swr^- Elo^+, produces flagella (Fla^+), and swims (Swm^+), emphasizing that FliL is essential for swarming but not for swimming motility. Significantly, the loss of *fliL* also abolishes the response of the cell to viscosity (in this case, the concentration of agar in nutrient medium), suggesting the role of FliL in surface sensing (34). YL1003 does not swarm on a surface, irrespective of the concentration of agar in the medium (34). An increase in the number of flagella per cell surface area is a hallmark of *P. mirabilis* swarmer cell differentiation induced after the cell has sensed a surface. An unexpected result of the *fliL* mutation in YL1003 is a decrease in expression of flagellin (encoded by *flaA*) (34), which further emphasizes the loss of surface sensing in *fliL* mutations. Paradoxically, expression of *flhD* and *fliA* increases in YL1003 (34). Disruption of *fliL* has also been reported to affect flagellar synthesis in other organisms: e.g., *Silicibacter* sp. strain TM1040 and *Pseudomonas putida* DOT-T1E (32, 36). Since FliL is a structural component of the flagellum, this outcome suggests that the *fliL* mutation in YL1003, but not necessarily the loss of FliL, has an unknown negative effect on the regulation of *flaA* (34). Insertion of the kanamycin cassette in the *fliL* gene may perturb the structure of the *fliL* operon mRNA in YL1003, which in turn may repress *flaA* transcription through an unknown mechanism.

To eliminate possible effects caused by the alteration of *fliL* DNA sequence, we describe here the construction and phenotype of a mutant with complete deletion of *fliL* (Δ*fliL*). We discovered that Δ*fliL* cells swarm but have defects in their surface-sensing mechanism, such that they swarm precociously on soft agar where the parent strain does not move. Unlike the wild-type parent, swarming of Δ*fliL* cells is also affected by temperature and is in-

TABLE 1 Bacterial strains and plasmids used in this study

Strain or plasmid	Relevant characteristics[a]	Source and/or reference
Strains		
P. mirabilis		
BB2000	Wild type; spontaneous Rf^r from PRM1	37
YL1006	BB2000 *fliL*Δnt 4–459 (encoding residues 2–153)	This study
E. coli		
DH5α λ*pir*	*supE44* Δ*lacU169* (ϕ*lacZ*ΔM15) *recA1 endA1 hsdR17 thi-1 gyrA96 relA1* λ*pir* phage lysogen	39
JW1928	BW25113 Δ*fliL790*::*kan* (nt 4–444 replaced by *kan*)	CGSC (41)
RP437	F$^-$ *thr-1 araC14 leuB6*(Am) *fhuA31 lacY1 tsx-78* λ$^-$ *eda-50 hisG4*(Oc) *rfbC1*? *rpsL136*(*strR*) *xylA5 mtl-1 metF159*(Am) *thiE1*	38
SM10 λ*pir*	*thi-1 thr leu tonA lacY supE recA*::*RP4-2*-Tc::Mu λ*pir* phage lysogen; Km^r	40
XL1-Blue	*recA1 endA1 gyrA96 thi-1 hsdR17 supE44 relA1 lac* [F′ *proAB lacI*^{q}ZΔM15 Tn*10* (Tc^r)]	Stratagene
YL102	RP437 *fliL* Δ*fliL790*::*kan*	This study
YL103	RP437 *fliL*Δnt 4–444 (encoding residues 2–148)	This study
Plasmids		
pACYC184	Cloning vector; p15A ori; Cm^r Tc^r	19
pCP20	Plasmid showing temperature-sensitive replication and containing yeast Flp recombinase gene, FLP; Ap^r Cm^r	45
pKNG101	Suicide vector, R6K ori; Sm^r	42
pYL30	pACYC184 containing 699-bp DNA fragment containing P_{fliL} (200 bp upstream from start codon), codon region, and 16-bp downstream *fliL*; Cm^r	34
pYL68	pACYC184 containing P_{flhD}::*lacZ* transcriptional fusion; Cm^r	This study
pYL70	pACYC184 containing P_{flaA}::*lacZ* transcriptional fusion; Cm^r	34
pYL73	pACYC184 containing P_{umoA}::*lacZ* transcriptional fusion; Cm^r	This study
pYL115	pKNG101 containing 3,389-bp fragment from 1,480 bp upstream through 1,426 bp downstream of *fliL* gene; Sm^r	This study
pYL117	pYL115 with deletion of nt 4–456 of *fliL* codon region; Sm^r	This study
pYL125	pACYC184 containing P_{fliA}::*lacZ* transcriptional fusion; Cm^r	This study
pYL126	pACYC184 containing P_{flaA}-*flaA′*::′*lacZ* translational fusion; Cm^r	This study
pYL128	pACYC184 containing P_{motA}::*lacZ* transcriptional fusion; Cm^r	This study

[a] Ap^r, Cm^r, Km^r, Rf^r, Sm^r, and Tc^r indicate ampicillin, chloramphenicol, kanamycin, rifampin, streptomycin, and tetracycline resistance, respectively.

hibited at low temperature, hinting that the loss of FliL causes a temperature-dependent depowering of the flagellar motor. A Δ*fliL* mutant strain of *E. coli* also constructed as part of this study phenocopies the *P. mirabilis* Δ*fliL* strain in being Swr$^+$ with an alteration in temperature-dependent motility.

MATERIALS AND METHODS

Bacterial strains and growth conditions. The bacterial strains and plasmids used in this study are listed in Table 1. *P. mirabilis* BB2000 (37) is the wild-type stain and the parent of all mutants used in this study. *P. mirabilis* YL1006 is a Δ*fliL* strain with a deletion between nucleotide (nt) positions 4 and 459 in the *fliL* gene (construction described below). *E. coli* RP437 (38) is the parent of YL102 and YL103. *E. coli* DH5α λ*pir* (39) and SM10 λ*pir* (40) were used for construction of pKNG101-derivated plasmids and biparental mating, respectively. *E. coli* JW1928 (obtained from the CGSC at Yale University) (41) is the donor of the Δ*fliL790*::*kan* allele used to construct *E. coli* Δ*fliL* strains (methods described below). *E. coli* XL1-Blue (Stratagene) was used for plasmid manipulations. *E. coli* and *P. mirabilis* were maintained in Luria-Bertani (LB) broth as described previously (34). LSW$^-$ agar (34) was used to acquire single colonies of *P. mirabilis*. As required, media were supplemented with 100 μg ml^{-1} ampicillin, 40 μg ml^{-1} chloramphenicol, 50 μg ml^{-1} kanamycin, 50 μg ml^{-1} streptomycin, or 15 μg ml^{-1} tetracycline. Swimming motility was screened and analyzed in tryptone broth (T broth: Bacto tryptone, 10 g liter^{-1}; NaCl, 5 g liter^{-1}) or Mot agar (T broth containing 3 g liter^{-1} Bacto agar).

Growth curves. A single colony was inoculated into 2 ml LB broth and incubated at 37°C with shaking (200 rpm) overnight. The overnight culture was mixed, and a 1:100 dilution was inoculated to fresh LB broth at a starting optical density at 600 nm (OD_{600}) of 0.05 and incubated at 37°C with shaking. The OD_{600} of the culture was measured every hour using a Beckman DU640 spectrophotometer.

Swimming and swarming motility assay. Swimming and swarming motilities were measured as previously described (34) with minor modifications. Mot agar was used for measurement of swimming motility. LB broth containing Bacto agar (0.3% to 2.5%) or Eiken agar (Eiken Chemical Co., Tochigin, Japan) (0.6%) plus 0.5% glucose was used to determine the swarming motility of *P. mirabilis* or *E. coli*, respectively. Swimming and swarming assays were conducted in an environmental chamber at 37, 30, or 25°C with 46% relative humidity.

Construction of the *P. mirabilis* Δ*fliL* mutant. An in-frame deletion of *P. mirabilis fliL* was constructed using homologous recombination. A 3,389-bp fragment harboring a region from 1,480 bp 5′ of the start codon to 1,426 bp 3′ of the *fliL* stop codon was amplified from BB2000 genomic DNA (extracted using the DNeasy blood and tissue kit manufactured by Qiagen) and ligated into the BamHI and XbaI sites in the suicide vector pKNG101 (42, 43), resulting in pYL115. Reverse PCR was used to construct a deletion at nucleotides (nt) 4 to 456 and to introduce an NcoI site in *fliL* on pYL115. Subsequently, the PCR product was digested with NcoI and circularized by ligation to yield pYL117. pYL117 was transferred into YL1006 via biparental mating between *E. coli* SM10 λ*pir*/pYL117 and BB2000, as previously described (37). The exconjugants were selected on LSW$^-$ agar containing streptomycin and tetracycline. Streptomycin-sensitive isolates resulting from a double crossover event were selected by *sacB* counterselection (43). The deletion of *fliL* was confirmed by PCR using combinations of primer pairs matching the flanking and the internal regions of the *fliL* gene. The primers used are listed in Table S1 in the

supplemental material. The resulting strain, called YL1006, contained a deletion of nt 4 to 459 in the *fliL* coding region, which was confirmed by sequencing.

Construction of the *E. coli* Δ*fliL* mutant. Deletion of *fliL* in *E. coli* RP437 was constructed by P1 transduction to replace the wild-type *fliL* allele with the Δ*fliL*::*kan* allele from JW1928, a single-gene-knockout strain in the Keio collection (41). The result was YL102 (Δ*fliL*::*kan*). The kanamycin-resistant cassette in YL102 was removed by FLP recombination target (FRT) recombination, which was achieved by the expression of the Flp recombinase (44) from pCP20 (45) and resulted inYL103 (Δ*fliL*). Each deletion was confirmed by PCR and sequencing.

Construction of transcriptional and translational fusion vectors. Transcriptional fusions between the promoter regions of *flhD*, *umoA*, *fliA*, and *motA* (respectively) and *lacZ* were constructed in pACYC184 by previously described methods (34). The resulting plasmids are called pYL68 (P_{flhD}::*lacZ*), pYL73 (P_{umoA}::*lacZ*), pYL125 (P_{fliA}::*lacZ*), and pYL128 (P_{motA}::*lacZ*). pYL68 harbors a transcriptional fusion between the *flhD* promoter (−499 to −1 with respect to the start codon of *flhD*) and *lacZ*. pYL73 is a transcriptional fusion between the *umoA* promoter (−497 to −1 with respect to the start codon of *umoA*) and *lacZ*. pYL125 carries a transcriptional fusion between the *fliA* promoter (−477 to +53 with respect to the start codon of *fliA*) and *lacZ*. A transcriptional fusion between the *motA* promoter (−498 to +24 with respect to the start codon of *motA*) and *lacZ* is carried on pYL128.

A translational fusion between *flaA* and *lacZ* (*flaA′*::′*lacZ*) on pACYC184 was constructed as follows. Two-step overlap extension PCR was used to fuse a region of *flaA′* from −386 to +30 relative to the *flaA* start codon, and a ′*lacZ* fragment comprising +31 through the stop codon of *lacZ*). The resulting PCR product was ligated into the BamHI and HindIII sites of pACYC184, producing pYL126.

Measurement of transcription or translation by LacZ activity. LacZ activity was measured to assess the expression of *flhD*, *fliA*, *flaA*, *motA*, or *umoA* in agar-grown cells. Plasmids carrying a *lacZ* fusion were transformed into BB2000 or YL1006 by electroporation (46). One hundred microliters of an overnight culture containing a reporter plasmid was spread on the surface of LB agar and incubated at 37°C, with cells harvested every hour thereafter for a period of 7 h. β-Galactosidase activity was measured using the Miller assay (47) as described previously (48).

Measurement of transcription by qRT-PCR. The procedures for RNA extraction, cDNA synthesis, and quantitative reverse transcription-PCR (qRT-PCR) are described by Lee et al. (34). RNA samples were obtained from 2.75-h cultures grown in LB broth with shaking (200 rpm) and 4.5-h cultures grown on LB agar at 37°C. Changes in gene expression were calculated using the threshold cycle ($2^{-\Delta\Delta CT}$) formula (49), with *rpoA* serving as the reference transcript.

Protein sample preparation and Western blotting. Protein samples were prepared using methods described previously (34), with minor changes. In brief, *P. mirabilis* cells were grown in LB broth or on the surface of LB agar at 37°C or 25°C. For samples prepared from broth culture, bacteria were harvested at 37°C for 2.75 h or at 25°C for 6 h, which were chosen as the times of maximum pseudoswarmer cell production (18). For samples prepared from agar cultures, bacterial cells were washed off every hour after incubation at 37°C or 25°C from the LB agar surface with 2 ml of 1× phosphate-buffered saline (PBS [pH 7.40]) (34). In both cases, the pellets were collected by centrifugation (6,000 rpm for 10 min at room temperature), washed with 1× PBS, and then resuspended in 1 ml of 1× PBS. Wide-bore tips were used to prevent shearing of the flagella. Whole-cell homogenates of the pellets were prepared using six cycles of sonication for 10 s each, followed by a pause on ice for 30 s. A bicinchoninic acid (BCA) protein assay (Pierce) was used to determine the concentration of protein in each sample, and 1 μg of total protein was applied to an Any kD Mini-protean TGX polyacrylamide gel (Bio-Rad). The resolved proteins were transferred to Hybond-P polyvinylidene difluoride (PVDF) membranes (GE Healthcare) and detected as previously described (34). Digital images of the blot were acquired using the scanner function of HP Officejet 4500. ImageJ software (National Health Institute) was used to determine the amount of protein in bands on the developed Western blots.

Fluorescent staining and microscopic analysis. Morphological changes and swarmer cell differentiation were assessed in LB broth and on soft LB agar (LB with 0.9% agar). Bacterial cells were harvested from LB broth and plates of soft LB agar every hour after incubation. Cells were fixed and fluorescently stained using previously described methods (34). Stained specimens were mounted in ProLong antifade (Invitrogen) and imaged using wide-field fluorescence microscopy with a Zeiss Axio Observer Z1 microscope using Zeiss filter sets, 10 shift free (F), 15 shift free (F), and 49 4′,6-diamidino-2-phenylindole (DAPI) shift free (E) and a Hamamatsu Orca-R2 charge-coupled device (CCD) camera. Acquired images were analyzed with Volocity 6.0.1 software (PerkinElmer). Channels for membrane and nucleoid staining were deconvolved using an iterative restoration function (with 25 iterations and a 98% confidence limitation). Color and contrast adjustment of processed images were done using Photoshop CS6 (Adobe).

Morphometric analyses of live bacterial cells were done using wet-mount suspensions viewed using phase-contrast light microscopy with an Olympus BX60 and a QImaging QCam CCD camera. Cell length was determined using a "skeletal length measurement" tool (Volocity), with 7 μm as the cutoff to define the minimum length of a swarmer cell (34). The mean and standard deviation of the cell length of each cell type and nonlinear fitting of the Gaussian distribution were calculated using Origin 9.0 software (OriginLab). A minimum of 500 cells were analyzed to determine the mean cell length for each population.

Measurements of swimming speed and behavior were obtained using an overnight culture grown in 2 ml T broth that was inoculated into fresh T broth at a 1:100 dilution and incubated with shaking (200 rpm) at 37°C for 5 h. The 5-h cultures were diluted in prewarmed T broth to an OD_{600} of 0.04 and quickly imaged. Videos of a ca. 5-s duration (~25 frames per s) were captured. The motion of individual cells within a field was determined using the "track objects" function (with a trajectory variation tracking model [Volocity]). At least 150 tracks for each sample were analyzed. The minimum criterion defining a tumble was the change in direction of at least 90°.

Drop collapse assay. A modification of the drop collapse assay of Be'er and Harshey (50) was used to determine the presence of surfactant in supernatants of bacterial cultures. One hundred microliters of an overnight culture was spread on the surface of soft LB agar and incubated at 37°C. At 5 h, the bacterial cells were scraped off the plate using a glass coverslip and resuspended in 200 μl deionized water, which was then transferred to a microcentrifuge tube. The cell pellet and the supernatant were separated by centrifugation at 8,000 rpm for 10 min at room temperature. Five microliters of the supernatant was carefully applied to the surface of a lid from a polystyrene petri dish (Fisher Scientific). After 1 min, a photograph of the side of the drop was taken with the camera lens parallel to the plastic surface. The contact angle, defined as the angle between the drop tangent contacting the plastic surface and the reflection line, was measured directly from the digital image using ImageJ software.

RESULTS

Δ*fliL* cells of *P. mirabilis* swarm. A mutant of *P. mirabilis* with 90% of *fliL* deleted (YL1006 [*fliL*Δnt 4–459]) was constructed (Materials and Methods). The growth of YL1006 is unaffected by the *fliL* mutation (see Fig. S1A in the supplemental material), and the deletion is nonpolar on the other genes in the *fliL* operon (see Fig. S1B). Based on previous experience with other $FliL^-$ mutants and the reports of *fliL* deletions in other bacteria (27, 34), we predicted that YL1006 would be Swr^-; however, these Δ*fliL* cells swarmed nearly the same as parental cells (Fig. 1A, right panel), while possessing minor defects in swimming (Fig. 1A, left panel). Similar to other *fliL* mutants of *P. mirabilis*, YL1006 is Elo^+, pro-

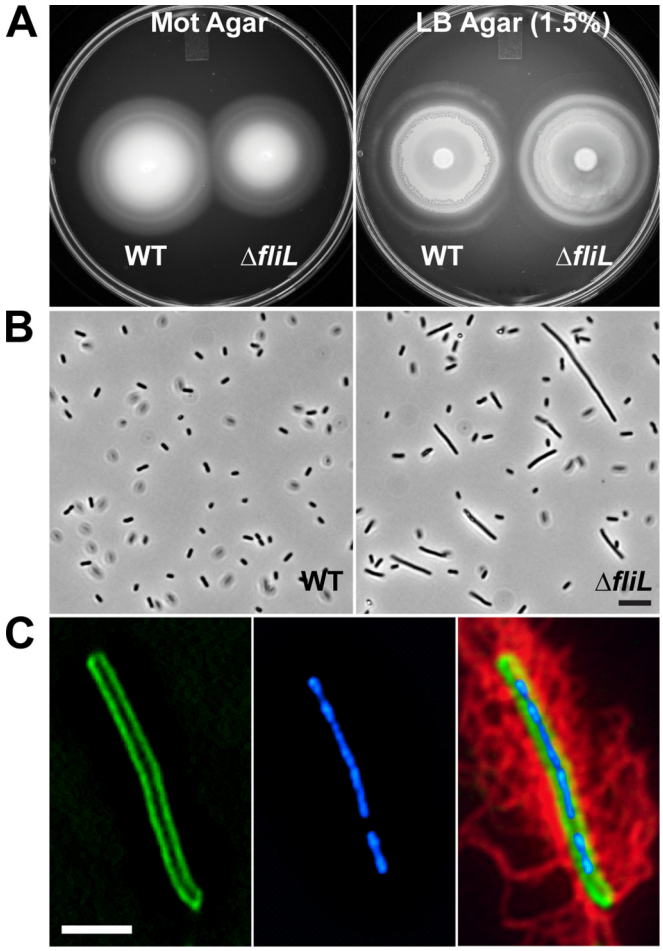

FIG 1 Phenotype of *P. mirabilis* Δ*fliL* strain YL1006. (A) Swimming and swarming motilities on Mot agar (left) and hard LB agar (right), respectively. (B) Phase-contrast micrographs of cells of broth-grown cells. Scale bar, 10 μm. WT, wild type. (C) A representative Δ*fliL* pseudoswarmer cell showing (from left to right) membrane (FM1-43 [green]), nucleoids (DAPI [blue]), and flagella (anti-FlaA immunostaining [red]). Scale bar, 5 μm.

ducing elongated cells in broth morphologically similar to pseudoswarmer cells seen in other *fliL* mutants (Fig. 1B). However, unlike YL1003, YL1006 pseudoswarmer cells are hyperflagellated (Fig. 1C; see Fig. S2 in the supplemental material) and for all purposes phenocopy wild-type swarmer cells obtained from agar. Thus, to distinguish them from YL1003 pseudoswarmer cells and wild-type agar-grown swarmer cells, we refer to the YL1006 cells as hyperflagellated pseudoswarmer cells (HPCs). Like other *fliL* pseudoswarmer cells, YL1006 HPC production is transient (with a maximum of 6.2% HPCs in the population at 2.75 h). As previously reported for other *fliL* pseudoswarmer cells, nucleoids in the Δ*fliL* HPCs are irregularly spaced, which implicates a function for FliL in cell septation and/or partitioning of the chromosome. These results show that FliL is not essential for *P. mirabilis* swarming.

Δ*fliL* cells precociously swarm on low-viscosity surfaces. Our previous results have implicated FliL in viscosity-dependent surface sensing (34), such that defects in *fliL* alter the cell's response to a surface. Swimming and swarming motility were examined in wild-type and YL1006 cells using LB broth containing different concentrations of agar, with the concentration of agar acting as a proxy for viscosity. We define "semisolid agar" as broth containing 0.3% agar: "soft" agar is broth with 0.9% agar, and "hard" agar contains 1.5% agar. The results of these analyses are shown in Fig. 2 (see Fig. S3 in the supplemental material). As shown in Fig. 2, YL1006 swarms proficiently on LB with agar at 0.9% or above. As expected, swarming declines as viscosity increases. As is true for wild-type cells, YL1006 does not swarm when the viscosity of the surface is <0.9% agar, presumably because at this viscosity flagella rotate normally and rotation is unimpaired, and thus the cells do not sense that this is a surface. These results show that swarming of YL1006 is viscosity dependent.

As can be observed in Fig. 2 (see Fig. S3 in the supplemental material), YL1006 initiates swarming earlier (precocious swarming) and swarms significantly faster (3.2×) than the wild type on soft agar, while the difference in swarming is much less when on hard agar, i.e., YL1006 swarms slightly faster (1.4×) than the wild type on 1.5% agar. On soft agar, the maximum migration rate for YL1006 is 17.0 ± 2.9 mm/h compared with 5.3 ± 0.9 mm/h for the wild type, and YL1006 starts swarming at 3 h, compared to 6 h for wild-type cells. We conclude that Δ*fliL* cells have enhanced swarming over low-viscosity surfaces that otherwise prevent swarming of the wild type.

Similar to the wild type, YL1006 is able to swim through an agar matrix when the concentration is reduced to 0.3%, but Δ*fliL* cells swim at a slower speed than do wild-type cells (Fig. 2, top left panel). Why is YL1006 less effective in swimming through semisolid agar than BB2000? One possibility is that the *fliL* defect decreases swimming speed or alters the swimming behavior of the cell. Such changes in the swimming speed and behavior of individual cells could affect overall migration through semisolid agar. This hypothesis was tested by measuring the speed and direction of live cells using microscopy and cell tracking analyses. As shown in Table 2, the average swimming speed of YL1006 is ca. 10% less than the speed of the wild type (14.2 compared with 15.6 μm/s), while the tumbling frequency of the mutant is slightly higher (12.9%) than that of the wild type (11.9%). These differences are not statistically significant but may subtly reduce the overall migration rate in semisolid agar. However, as shown in Fig. 3, YL1006 cultures contain a higher percentage of poorly motile cells (61.0%) than do cultures of BB2000 (46.1%): i.e., the number of Δ*fliL* cells that swim fast decreases, while the percentage of cells that swim slowly increases (Fig. 3). These results suggest that the *fliL* defect in YL1006 reduces swimming speed, resulting in a population skewed toward more slowly swimming cells and helps explain why Δ*fliL* hampers swimming through semisolid agar.

Δ*fliL* results in a minor increase of *flaA* expression on soft agar. Why does YL1006 swarm proficiently over soft agar when BB2000 does not? Answers to this question are particularly important to our understanding of FliL's function, as paradoxically the same mutation hampers motility in lower-viscosity environments (i.e., semisolid agar). In approaching this problem, we note that bacteria employ common strategies to overcome the lack of wetness and friction associated with a surface that include producing wetting agents (surfactants), increasing the number of flagella, and increasing the length of the cell (51). The *fliL* mutation may affect any one of these factors to promote YL1006 swarming over soft agar.

We assessed surfactant production using a drop collapse assay,

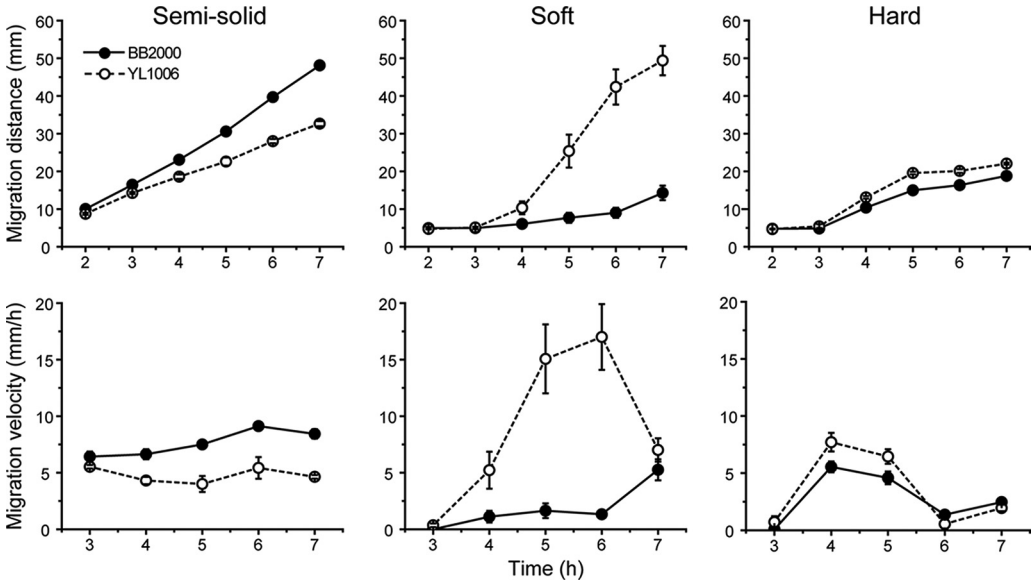

FIG 2 Comparison of wild-type and Δ*fliL* mutant cell motilities as affected by the concentration of agar in the medium. Shown is migration of the wild-type (solid circles) and Δ*fliL* (open circles) cells on LB with 0.3% (semisolid), 0.9% (soft), and 1.5% (hard) agar. (Top row) Migration distance; (bottom row) migration velocity. Means ± standard deviations from three independent experiments are shown.

in which a reduction in contact angle of the drop is correlated with more surfactant. As shown in Fig. S4 in the supplemental material, the contact angles between drops of supernatant from wild-type cells (contact angle of 71°) and Δ*fliL* cells (contact angle of 72°) are the same within the detection limits of this assay. Therefore, the *fliL* mutation has no demonstrable effect on surfactant production, and both YL1006 and wild-type cells produce the same amount of wetting agent, ruling out surfactant production as a cause of YL1006 swarming over soft agar.

To test if an increase in flagella allowed Δ*fliL* cells to swarm over soft agar, we measured flagellin (*flaA*) expression in cells grown on soft agar and found that wild-type and Δ*fliL* cells have nearly identical levels of expression of *flaA* during the time period between 1 h and 4 h after inoculation (Fig. 4A). As the incubation progressed beyond 4 h, a difference in *flaA* transcription became noticeable: e.g., wild-type *flaA* expression was higher (1.3×) than *flaA* expression in YL1006, and *flaA* transcription remained higher in wild-type cells for the remainder of the time course.

A more dramatic difference was seen when comparing translation of *flaA* in wild-type and Δ*fliL* cells (Fig. 4B). Mirroring the transcription data, from 1 to 3 h after inoculation, translation of *flaA* increases dramatically in both YL1006 and BB2000, with *flaA* translation in Δ*fliL* cells increasing faster than the rate in wild-type cells (3.9× versus 2.5× from the 2-h to 3-h time points). After this, *flaA* translation leveled out; it ultimately declined at the end of the time course (7 h) and was ca. 1.4× greater in Δ*fliL* cells than in wild-type cells (Fig. 4B).

TABLE 2 Analysis of swimming motilities of BB2000 and YL1006 cells at 37°C

Strain	Swimming speed (μm/s)	Tumbling rate (%)	% of motile cells
BB2000 (wild type)	15.5 ± 2.5	11.9	46.1
YL1006 (Δ*fliL* mutant)	14.2 ± 3.0	12.9	61.0

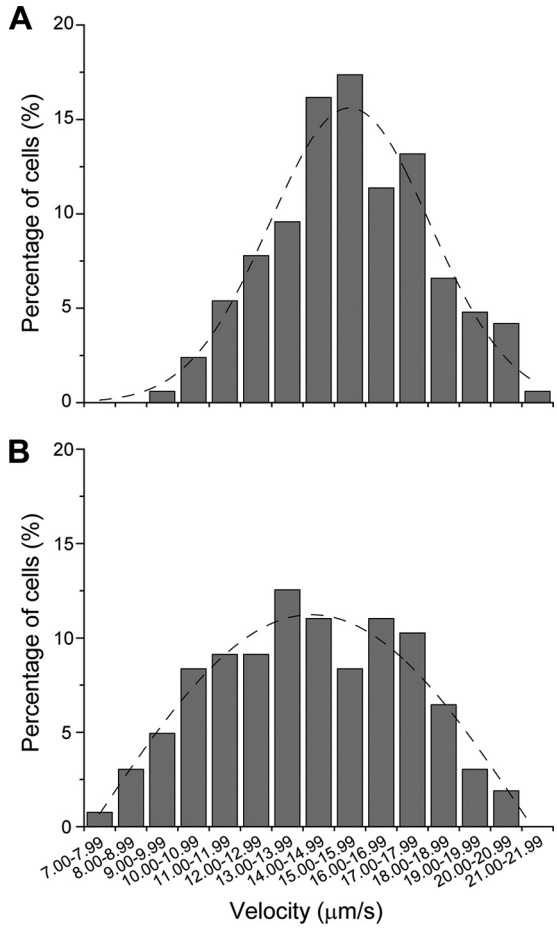

FIG 3 Comparison of swimming speeds between wild-type and Δ*fliL* mutant populations. Shown is a histogram of the percentage of swimming cells of the wild-type (A) versus the Δ*fliL* mutant (B). The dashed line in each panel is a nonlinear fitting of the Gaussian distribution of the data in each graph.

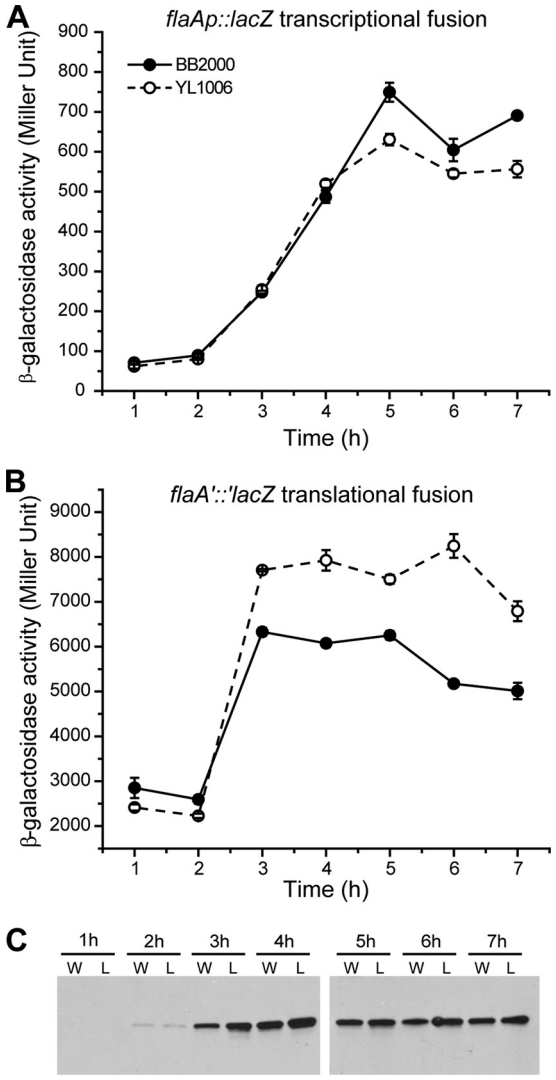

FIG 4 Expression of flagellin (FlaA) in wild-type and Δ*fliL* mutant cells. Shown are transcription (A) and translation (B) of *flaA*, measured as β-galactosidase activity from a P_{flaA}::*lacZ* transcriptional fusion and *flaA*′::′*lacZ* translational fusion, respectively, in wild-type (solid circles) and Δ*fliL* (open circles) cells. Means ± standard deviations are shown ($n = 3$). (C) Immunoblot to flagellin in wild-type (W) and Δ*fliL* (L) cells.

Flagellin production parallels *flaA* translation and is very low (almost undetectable) prior to 3 h, after which flagellin significantly increases (Fig. 4C). Comparable to *flaA* translation, after 3 h, FlaA protein in Δ*fliL* cells was 1.2 to 1.4× higher than that in wild-type cells (Fig. 4C). While the shapes of the transcription and translation curves (respectively) and overall patterns of flagellin protein levels are similar in YL1006 and wild-type cells, increased translation of *flaA* and FlaA levels in YL1006 are evident. We conclude that YL1006 produces more flagella than wild-type cells on soft agar, and this increase promotes precocious swarming.

Δ*fliL* enhances cell elongation and *umoA* transcription on soft agar. Expression of *flaA* is dependent upon $FlhD_4C_2$ and FliA and increases along with the expression of other class 3 transcripts, such as *motA* and *umoA*. Does the *fliL* mutation in YL1006 affect the expression of other class 3 transcripts when cells are swarming over soft agar? We compared the levels of expression of four genes (*flhD*, *fliA*, *motA*, and *umoA*) in YL1006 and BB2000 cells grown on soft agar. Overall, the kinetics of expression of *flhD* (class 1 promoter), *fliA* (both class 2 and 3 promoters), *motA* and *umoA* are similar to those of *flaA* (compare Fig. 4 and 5), with the exception that transcription of these four genes decreases between 5 and 6 h, whereas *flaA* expression does not. Expression of *umoA* is markedly higher (2 to 5×) in YL1006 compared with the wild type (Fig. 5D). An equivalent increase in *umoA* transcription was also detected in broth-grown Δ*fliL* cells (Table 3) (18). qRT-PCR analysis showed that transcription of *flhDC* in broth-grown cells at 2.75 h (when YL1006 produces the maximum number of HPCs) is not different from that of the wild type (data not shown). Since the function of *umo* genes is thought to take part in *flhDC* expression, we measured the expression of *umoB* and *umoD*, which are also involved in swarming motility (26). As observed with *umoA*, *umoD* expression increased in Δ*fliL* cells compared with wild-type cells, but by a smaller amount (1.1 to 1.5×), while *umoB* expression remained unchanged (Table 3). These data suggest an indirect role of FliL in the control of *umoA* and *umoD* expression. We conclude that the expression of *umoA* and *umoD* is upregulated when Δ*fliL* cells swarm on soft agar and helps to explain precocious swarming.

Our third hypothesis to explain why YL1006 swarms on soft agar is that the *fliL* mutation causes an increase in the length of the cell or in the number of swarmer cells in the population. Using phase-contrast microscopy of living cells obtained from soft agar, we found that swarmer cells (i.e., cells >7 μm in length) comprised 10.8% of the YL1006 population, while only 3.4% of wild-type cells were swarmer cells (Fig. 6A). The population of YL1006 cells grown on soft agar also produces ca. 3× more preswarmer cells (defined as those cells with lengths between 4 and 7 μm) during the first 3 h of growth (Fig. 6B). Thus, a Δ*fliL* population swarming on soft agar has 3× more swarmer cells and 3× more preswarmer cells than its wild-type counterpart. While there are more swarmer cells in YL1006 populations grown on soft agar, there is no statistical difference in the mean cell lengths of Δ*fliL* and wild-type swarmer cells: the YL1006 swarmer cell length is 12.18 ± 3.13 μm, while wild-type swarmer cells average 10.42 ± 2.86 μm. These results suggest that Δ*fliL* cells swarm on soft LB agar by increasing the number of swarmer cells aided by precocious swarmer cell development.

Δ*fliL* results in a low-temperature inhibition of swarming. While conducting experiments with YL1006, we observed that, unlike in the wild type, Δ*fliL* cells failed to swarm on hard agar when left on the lab bench at room temperature. This observation was further explored, and the results are shown in Fig. 7. Although Δ*fliL* cells swarm on hard agar at 37°C, unlike BB2000, their swarming is inhibited at temperatures below 37°C. YL1006 has a significant reduction in swarming at 30°C (Fig. 7, middle panel) and completely loses the ability to swarm over hard agar at 25°C (Fig. 7, lower panel). One explanation for the failure of YL1006 to swarm at 25°C is that low temperature may prevent swarmer cell differentiation. This is not the case, as Δ*fliL* cells grown at 25°C produce HPCs in broth and differentiate into normal swarmer cells on hard agar (Fig. 8A). The percentage of YL1006 HPCs and swarmer cells produced at 25°C is roughly equal to those produced at 37°C. When in broth cultures, 5.6% of the YL1006 population are HPCs, while on hard agar, 36% of the cells are differentiated swarmer cells. At 25°C, the number of flagella per μm of

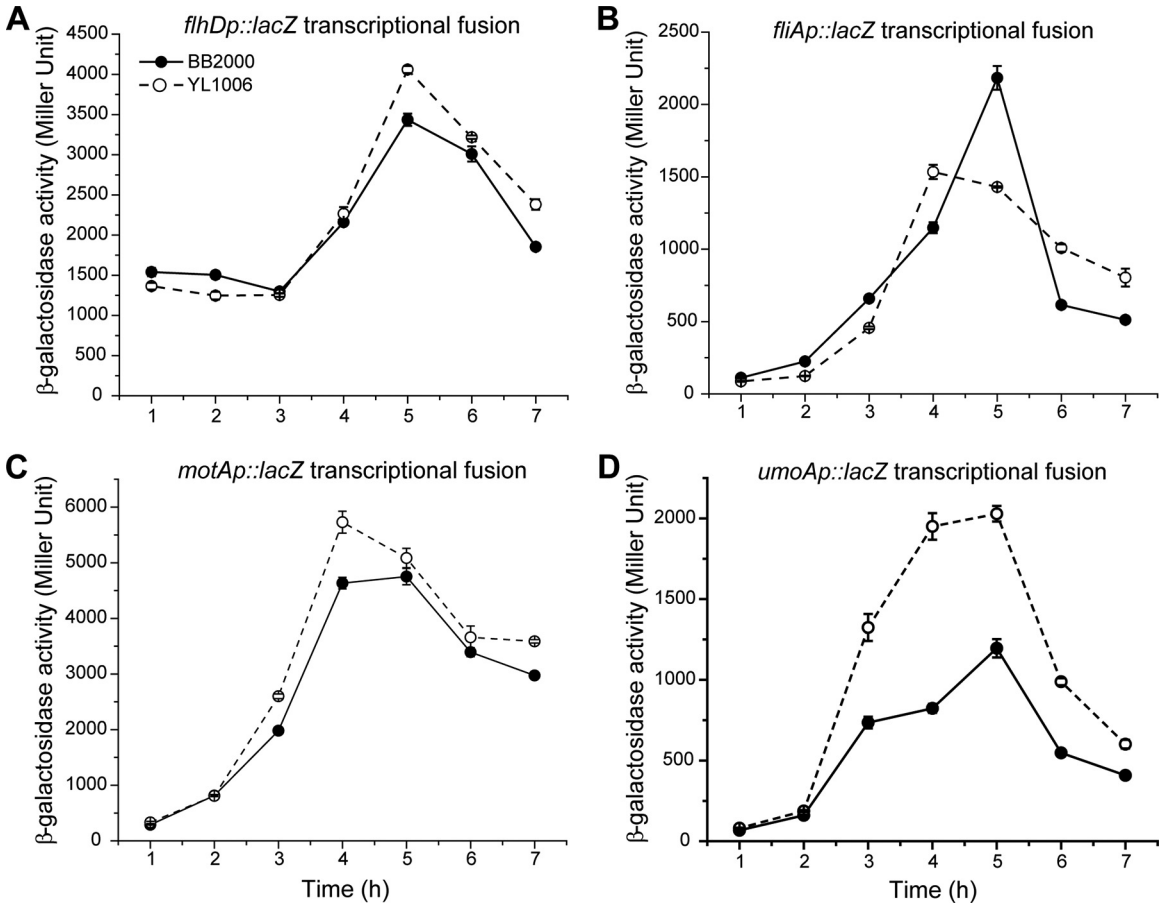

FIG 5 Comparison of the levels of expression of *flhD*, *fliA*, and *motA* in wild-type (solid circles) and Δ*fliL* (open circles) cells. Transcription of *flhD* (A), *fliA* (B), *motA* (C), and *umoA* (D) in cells grown on soft LB agar was measured as β-galactosidase activity from their respective *lacZ* transcriptional fusions. Means ± standard deviations ($n = 3$) are shown.

cell surface on either HPCs or swarmer cells is the same as when grown at 37°C, and Δ*fliL* cells have wild-type production of flagellin at the lower temperature (Fig. 8B). These results lead us to conclude that inhibition of YL1006 swarming at low temperature is not due to defects in swarmer cell differentiation or flagellar synthesis. Another possible explanation for the lack of swarming is that the flagella of Δ*fliL* cells are more fragile at 25°C; however, this is not the case, as we did not detect a significant amount of detached flagellin by Western blotting in the supernatant fraction harvested from the agar surface (data not shown).

We questioned whether low temperature also inhibits motility of Δ*fliL* cells on semisolid agar, which would suggest that loss of FliL in YL1006 may somehow deenergize the flagellar motors. The results are shown in Table 4 and in Table S2 in the supplemental material. In general, Δ*fliL* cells are poorer swimmers than wild-type cells, irrespective of temperature, and swim at ca. 70% the speed of wild-type cells at 37°C (Table 4). At 25°C, Δ*fliL* cell swimming is further reduced to ca. 30% of the wild-type rate (Table 4; see Table S2). As can be seen in Table 4, while the mean migration velocity of wild-type cells in semisolid agar at 25°C is 30% of the swimming speed of the same strain at 37°C (2.2 ± 0.2 versus 7.4 ± 1.6 mm/h), incubation at the lower temperature has a much greater effect on Δ*fliL* cells than it does on wild-type cells (0.7 ± 0.3 versus 5.0 ± 0.7 mm/h), reducing the swimming speed of Δ*fliL* cells at 25°C to ca. 14% of the velocity at 37°C. We conclude that the flagellar motors of Δ*fliL* cells are more negatively affected at 25°C than are the motors of wild-type cells and suggest that these results support a role for FliL in flagellar motor performance or energetics.

TABLE 3 Fold change in expression of *umoA* and *umoD* in YL1006 compared with BB2000 cells in broth- or soft surface-grown cultures

Gene	Broth		Agar	
	Fold change in expression[a]	*P* value	Fold change in expression[a]	*P* value
umoA	1.8 ± 0.4	0.10	1.8 ± 0.4	0.05
umoB	0.9 ± 0.1	0.14	0.9 ± 0.1	0.15
umoC	ND[b]	NA[c]	ND	NA
umoD	1.1 ± 0.1	0.21	1.5 ± 0.3	0.04

[a] The fold change in expression (YL1006 versus BB2000) was calculated to compare the expression of each gene (relative to the expression of *rpoA*, the reference gene) in YL1006 (the Δ*fliL* mutant) with the expression of the same gene (relative to *rpoA* expression) in BB2000 (the wild type). A value of >1 indicates that expression of the gene is greater in YL1006 than in BB2000, while a value of <1 means that expression decreases in YL1006. Means ± standard deviations from three independent measurements from three biological samples are presented.
[b] ND, not done.
[c] NA, not applicable.

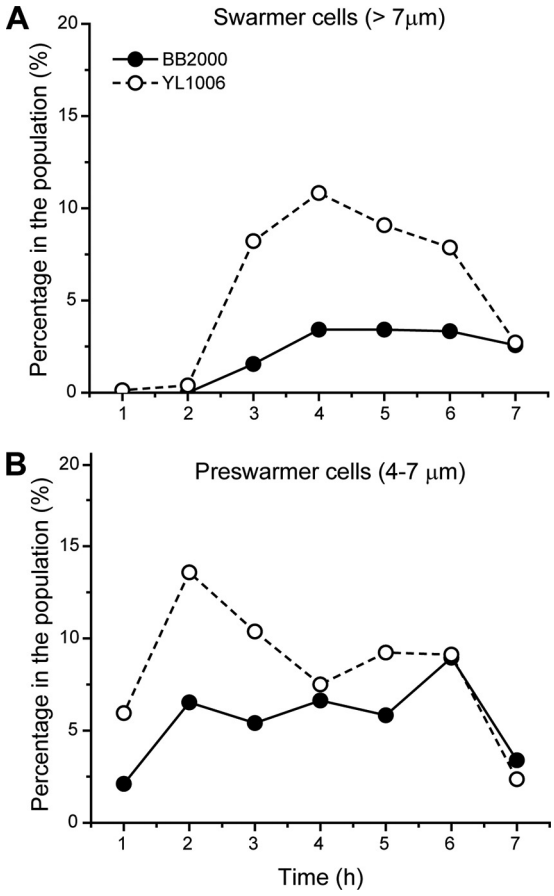

FIG 6 Comparison of rates of swarmer cell synthesis in wild-type and Δ*fliL* populations grown on soft LB agar. The percentages of swarmer cells (>7 μm) (A) and preswarmer cells (4 to 7 μm) (B) in the entire population ($n > 500$) were examined.

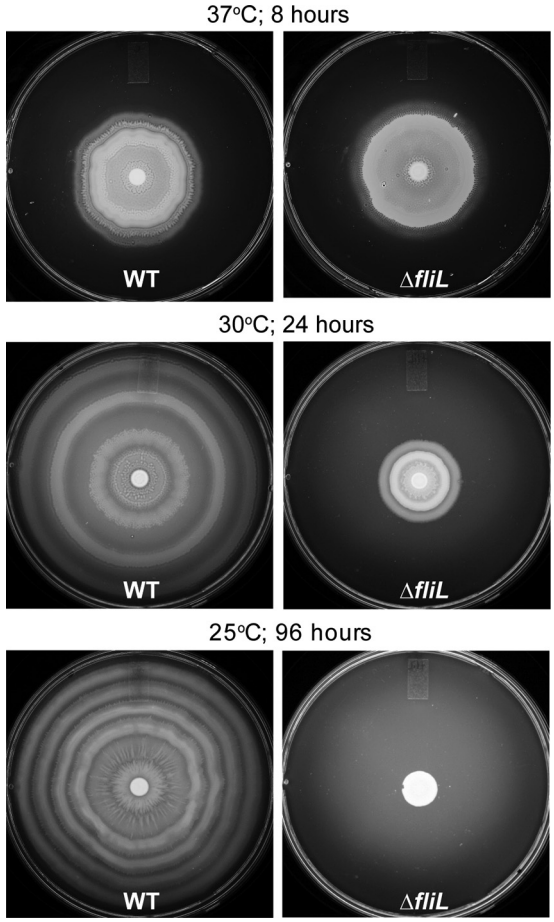

FIG 7 Effect of incubation temperature on the swarming of wild-type and Δ*fliL* mutant strains on hard LB agar.

***fliL*$^+$ in *trans* partially complements the Δ*fliL* phenotype.** Three phenotypic characteristics are unique to Δ*fliL* cells: (i) the production of HPCs, (ii) precocious swarming on soft agar, and (iii) low-temperature inhibition of swarming. We asked whether *fliL*$^+$ in *trans* could complement the YL1006 *fliL* mutation and return the Δ*fliL* phenotype to wild type. Plasmid pYL30, containing *fliL* under the control of its native promoter, was introduced into YL1006, and the resulting phenotype was determined (Fig. 9).

First, YL1006/pYL30 cells lost their ability to form HPCs in broth and resembled wild-type swimmer cells (Fig. 9A), demonstrating that a functional FliL complemented the Δ*fliL* mutation and prevented HPC formation by Δ*fliL* cells. Second, on soft agar *fliL*$^+$ complemented the *fliL* mutation, and YL1006/pYL30 cells swarmed the same as wild-type cells, losing their precocious swarming nature (Fig. 9B, middle panel). In conducting these experiments, we consistently observed that expression of *fliL*$^+$ in *trans* resulted in a marked decrease in both swimming and swarming over all surfaces tested (Fig. 9B). Inhibition of motility is most pronounced when the cells are swarming, with a 40 to 80% reduction in swarming compared with a 10% reduction in swimming migration. One reason for the decrease in motility is that expression of *fliL*$^+$ in *trans* results in a decrease in flagella (Fig. 9C) and occurs when *fliL* is driven from either its native promoter or a heterogenous promoter, such as P_{trc} (data not shown).

The third phenotype of Δ*fliL* cells, inhibition of swarming at low temperature, was not altered by expression of *fliL*$^+$ *in trans*. We suspect that this is due to repression of flagellar synthesis when *fliL*$^+$ is expressed from a plasmid (as shown in Fig. 9C). We conclude that while expression of *fliL*$^+$ in *trans* does not fully recapitulate the wild-type phenotype, two of the three unique phenotypes of YL1006 are complemented. Furthermore, these results point to an unexpected repression of motility and flagellar production by expression of *fliL*$^+$ *in trans*.

***E. coli* Δ*fliL* partially phenocopies *P. mirabilis* Δ*fliL*.** Many reports, including our previous papers, have underscored the importance of *fliL* in swarming, not just in *P. mirabilis*, but in other enteric bacteria as well (8, 27, 34). We wondered if the Swr$^+$ phenotype that we observed in YL1006 is unique to *P. mirabilis* or if instead it is more universal and apparent in other enteric bacteria. This was tested by constructing an *E. coli* Δ*fliL* strain with a nearly identical in-frame deletion to that in *P. mirabilis* YL1006. The result is *E. coli* YL103 (*fliL*Δnt 4–444), a strain that swarms well (Fig. 10). Furthermore, like *P. mirabilis* YL1006, loss of *fliL* in YL103 results in altered temperature effects on motility. For both *P. mirabilis* and *E. coli*, loss of *fliL* enhances swarming at 37°C (Fig. 10). For YL103, loss of *fliL* results in a >220% increase in swarming at 37°C (compared to the wild-type control). This result suggests that *fliL*$^+$ may repress motility of *E. coli*, similar to that ob-

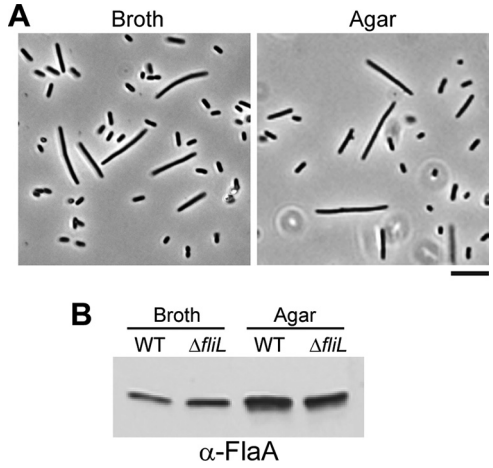

FIG 8 Cell morphology and flagellin expression of wild-type and Δ*fliL* mutant cells at 25°C. (A) Phase-contrast micrographs (400× magnification) of Δ*fliL* cells obtained from LB broth after 6 h or hard LB agar at 8 h of growth at 25°C. Scale bar, 10 μm. (B) Immunoblot to flagellin in the wild-type (WT) and Δ*fliL* cells grown in LB broth for 6 h or LB agar for 8 h.

served in *P. mirabilis*. Indeed, as shown in Fig. 11, expression of *fliL*$^+$ in *trans* also inhibits swarming of *E. coli* Δ*fliL* cells. On the other hand and unlike what we observed with *P. mirabilis* Δ*fliL* cells, growth of YL103 at lower temperatures (i.e., 30°C and 25°C) results in more moderate to no effects. We conclude that *E. coli* Δ*fliL* partially phenocopies *P. mirabilis* Δ*fliL*. This result emphasizes the universal nature of the Δ*fliL* phenotype in enteric bacteria.

DISCUSSION

In this study, we investigated the function of *fliL* in *P. mirabilis*. We discovered that (i) cells without *fliL* are able to swarm (Swr$^+$), (ii) loss of *fliL* alters *P. mirabilis* sensing of surfaces, (i.e., a Δ*fliL* cell is more responsive to low-viscosity agar), (iii) loss of *fliL* enhances *P. mirabilis* swarmer cell differentiation (i.e., more swarmer cells are produced through precocious differentiation, and (iv) the motility of cells lacking *fliL* is temperature dependent.

It came as a surprise to find that Δ*fliL* cells of *P. mirabilis* swarm on hard agar at 37°C (Fig. 1A), as the phenotype of our previous *fliL* mutants—for example, YL1003 (*fliL*::*kan*-nt 30), an FliL null mutant—is Swr$^-$ (34). Why would the two *fliL* mutations result in opposite swarming phenotypes? These two *fliL* strains were constructed using different genetic manipulations that affect the *fliL* coding sequence in different ways. YL1003 has a nonpolar group II intron insertion (TargeTron) between nucleotides 30 and 31 of *fliL* and retains all of the *fliL* DNA (34), while YL1006 has a deletion of most of the *fliL* gene. It is apparent that these two mutations have different effects on flagellar synthesis, such that YL1006 produces HPCs reminiscent of wild-type swarmer cells, while flagellin synthesis is reminiscent of swimmer cell levels in YL1003 (Fig. 1C; see Fig. S2 in the supplemental material) (34). Why then is flagellar synthesis affected in YL1003 but not in YL1006? Expression of *flaA* and flagellin is significantly reduced in YL1003 (34), yet they are expressed at wild-type levels in YL1006 (Fig. 4), and both *fliL* mutants are incapable of synthesizing a functioning FliL protein. These facts lead us to conclude that the defects in swarming and flagellin expression observed in YL1003 are not due to the loss of FliL protein itself but rather are due to the presence of *fliL* DNA sequence. We speculate that swarming is wild type in YL1006 due to the loss of *fliL* DNA sequence that otherwise results in repressed flagellar synthesis. This idea is supported by our current results in both *P. mirabilis* and *E. coli* showing that in *trans* expression of *fliL*$^+$ inhibits motility and flagellin synthesis (Fig. 9 and 11). Thus, we hypothesize that *fliL* has two functions. First, the gene encodes the FliL protein, whose function will be discussed subsequently. Second, *fliL* DNA (or possibly *fliL* mRNA) has a regulatory function that, when present, directly or indirectly represses *flaA* expression. This finding suggests that some *fliL* mutants constructed in other laboratories may give results similar to YL1003 and mislead us about the function of FliL. We conclude that the *fliL* gene but not the FliL protein is essential for *P. mirabilis* swarming over hard agar.

FliL is also not necessary for *E. coli* swarming, a result that is counter to the reports of others (27). The Swr$^+$ phenotype of *E. coli* Δ*fliL* strain YL103 is reproducible, and the mutation with its associated Swr$^+$ phenotype has been reconstructed several times in independent experiments in our laboratory (data not shown), emphasizing that this characteristic is not due to second site mutations or other spontaneous events that could have led to a Swr$^+$ phenotype. What is the difference between YL103 and other *E. coli* Δ*fliL* strains, such as UA332 (27), that are Swr$^-$? The size and the location of the deleted region within *fliL* are the major differences that distinguish these strains. YL103 deletion removes nt 4 to 444 (of 465 nucleotides) in *fliL*, while UA332 has a smaller deletion (Δnt 61–402) (27). We hypothesize that the additional DNA sequence of the *fliL* allele in UA332 may be causing its Swr$^-$ phenotype by causing defects in flagellin expression as we observed in *P. mirabilis* YL1003.

It has been proposed in our previous studies that *P. mirabilis* FliL plays a role in sensing surfaces via the effect of medium viscosity on impaired flagellar motor function (34). Our present results further support this function. We have demonstrated in this work that Δ*fliL* cells have an altered response to viscosity. Importantly, Δ*fliL* cells do not lose their ability to sense viscosity or respond to surfaces, but rather loss of *fliL* changes the low-end threshold of the response to a "surface": e.g., the "window" of surface sensing is expanded to now include low-viscosity environments that normally are not sensed by wild-type *P. mirabilis*, resulting in a Δ*fliL* cell that responds to a greater range of viscosities. At the same time, the high end of the surface-sensing response of Δ*fliL* cells remains the same as that in wild-type cells.

TABLE 4 Migration velocity of BB2000 and YL1006 on semisolid LB agar

Strain	37°C			25°C		
	Migration velocity (mm/h)	Δ*fliL* mutant/wild-type ratio	*P* value	Migration velocity (mm/h)	Δ*fliL* mutant/wild-type ratio	*P* value
BB2000 (wild type)	7.4 ± 1.6			2.2 ± 0.2		
YL1006 (Δ*fliL* mutant)	5.0 ± 0.7	0.7	7.15E−04	0.7 ± 0.3	0.3	3.23E−07

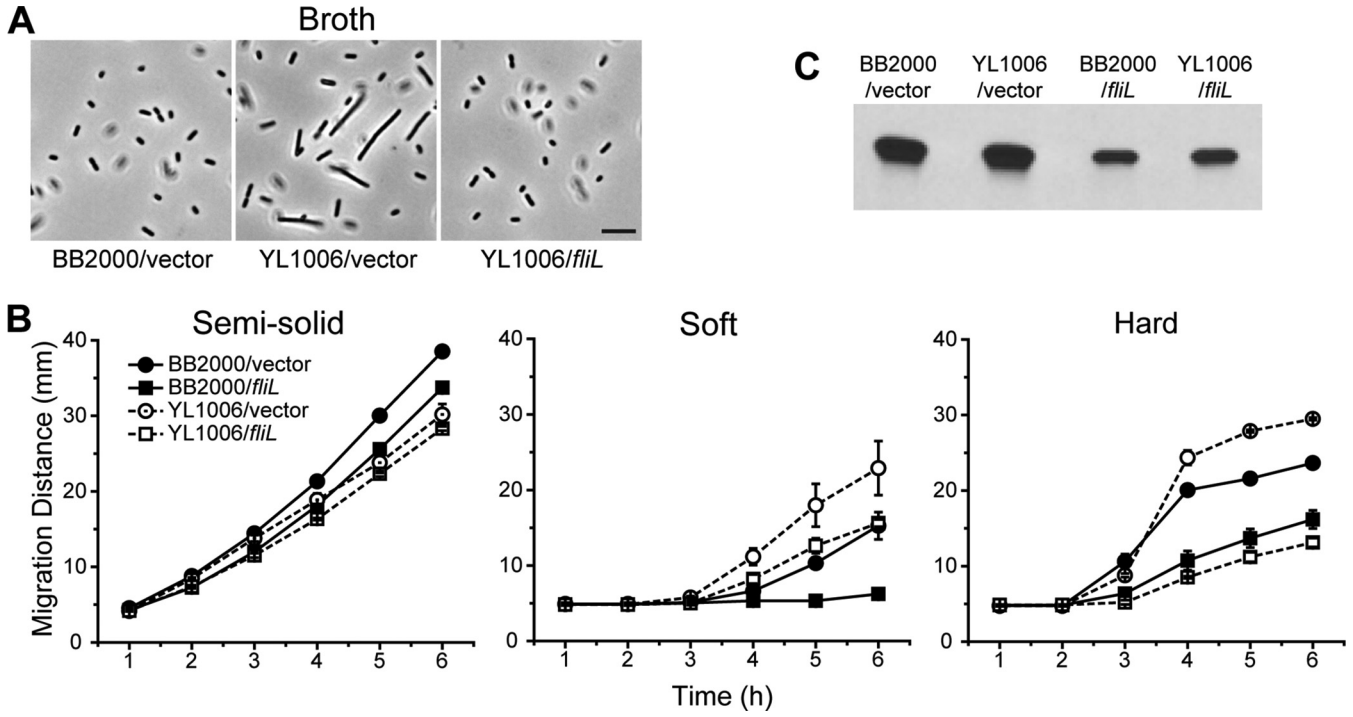

FIG 9 Cell morphology, migration, and flagellin production of wild-type and Δ*fliL* mutant cells affected by *fliL*$^+$. (A) Phase-contrast micrographs of wild-type and Δ*fliL* cells containing the empty cloning vector and *fliL* expressed in *trans*. Scale bar, 10 μm. (B) Migration of wild-type and Δ*fliL* cells as affected by the agar concentration in the presence and absence of *fliL*. Shown are the migration distances of the wild-type (solid symbols) and Δ*fliL* (open symbols) cells containing the empty cloning vector (circles) and *fliL* expression plasmid (squares) on semisolid, soft, and hard LB agar. Means ± standard deviations from three independent measurements are shown. (C) Comparison of flagellin production in wild-type and Δ*fliL* cells in the presence and absence of *fliL*. Shown is an immunoblot to flagellin in wild-type (BB2000) and Δ*fliL* (YL1006) cells containing empty cloning vector grown on the surfaces of soft LB agar at 37°C for 5 h.

What is the connection between the Δ*fliL* mutation and enhanced cellular differentiation of HPCs? Our results suggest that $FlhD_4C_2$ plays a central role in this differentiation process (16). The phenotype of *P. mirabilis flhDC*-overexpressing strains has been reported by the Hughes (University of Cambridge) and Rather (Emory University) groups (16, 24, 52). In these studies, overexpression of *flhDC* resulted in a reduction in the swarming lag period (what we call "precocious" swarming) and enhanced swarming motility, which was due to an increased expression of flagellin and elongated swarmer cells (16, 24, 52). Additionally, heightened amounts of $FlhD_4C_2$ give rise to swarmer-like cells (what we call "HPCs") in broth. The phenotype of a cell that overexpresses *flhDC* is identical to that of Δ*fliL* cells and suggests that control of $FlhD_4C_2$ is the endpoint of the FliL surface-sensing pathway. In support of this, previous results (34) and the present report clearly show that *flhD* expression increases in *fliL* mutants (Fig. 5). Similar to *flhD* expression, expression of *umoA* and *umoD* is also upregulated in Δ*fliL* cells (Table 3). Dufour et al. have shown that overexpression of *umo* genes induces differentiation of swarmer cells, suggesting that *umoA* (and perhaps *umoD*) plays a role in the swarmer cell elongation (25). Moreover, other *P. mirabilis fliL* mutants (e.g., BB2204, YL1001, and YL1003) have increased *umoA* expression (18), suggesting the role of FliL in the *umoA* signaling pathway. Since FliL is not a DNA-binding regulatory protein, changes in gene expression caused by the Δ*fliL* mutation are most likely due to indirect, downstream effects leading to control of *flhDC*. Our data implicate UmoA and UmoD as being two proteins that function in the surface-sensing pathway. In support of our hypothesis, Morgenstein and Rather have suggested UmoB and UmoD are involved in activation of the Rcs system that acts to control swarming (26). Furthermore, we have shown that mutations in the Rcs system, specifically those in *rcsC* or *rcsD* (formerly *rsbA*), result in an Elo$^+$ cells and precocious swarming (22) that partially phenocopy Δ*fliL* cells. The similarity between these mutant phenotypes suggests a possible involvement of the Umo proteins and the Rcs system in the FliL-mediated surface-sensing pathway.

As can be seen in Fig. 2, the loss of FliL has effects on swimming motility, such that the motility of Δ*fliL* cells in semisolid agar is slower than that of wild-type cells (see Fig. S3 in the supplemental material). The results from the present study suggest that the impairment of swimming results from a decreased number of fast-swimming motile Δ*fliL* cells (Fig. 3) that tumble more than wild-type cells (Table 2). However, other possibilities exist to explain the decrease in Δ*fliL* swimming, and they include the following: (i) the loss of FliL may cause slight structural defects in the HBB, and (ii) multiple flagellar filaments on Δ*fliL* HPCs may impair swimming motility due to tangling and ineffective coordination of multiple filaments. These factors undoubtedly contribute to the decrease in YL1006 overall migration.

In understanding the role FliL plays in surface sensing and flagellar motor function, it is important to emphasize two important findings from this study. First, there is the marked difference in response to viscosity displayed by Δ*fliL* cells compared to wild-type cells. This is best seen by comparing the swimming of Δ*fliL* cells to that of BB2000 in media with different viscosities. In very-

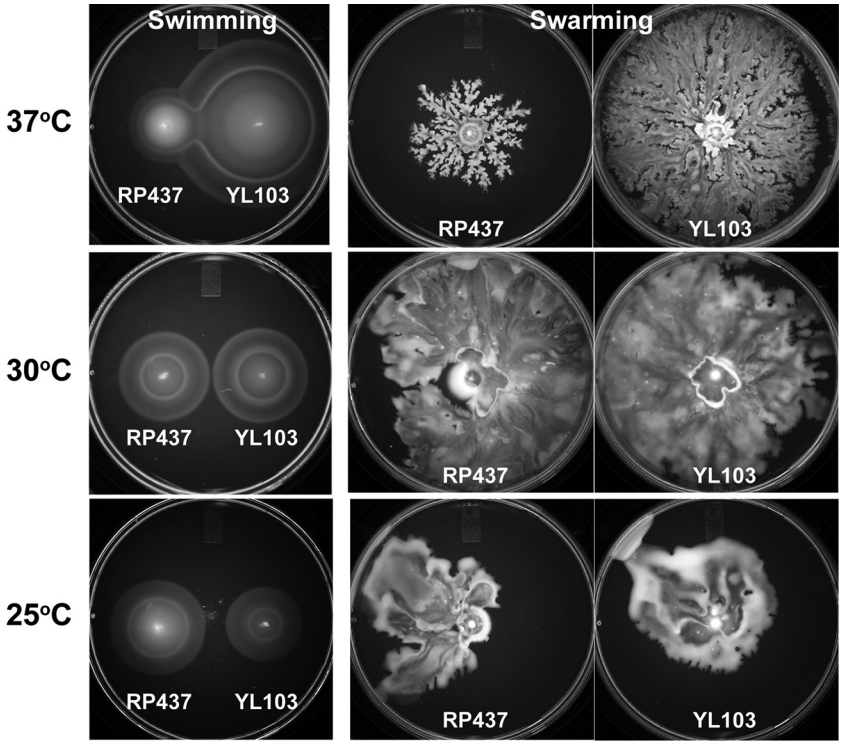

FIG 10 Swimming and swarming characterization of wild-type (RP437) and Δ*fliL* (YL103) *E. coli* cells. Swimming was measured on semisolid Mot agar, and swarming was measured on LB agar containing 0.6% Eiken agar and 0.5% glucose. Swimming plates were incubated for 8 h at 37°C and 30°C and for 24 h at 25°C. Swarming plates were incubated for 24 h at all temperatures.

low-viscosity nutrient broths (LB or T broth, for example), Δ*fliL* cells are only 10% slower than the wild type, but when the viscosity of the liquid is increased, as in semisolid agar, swimming of the Δ*fliL* mutant was markedly reduced (30% slower) compared with its parent. This suggests that the loss of FliL adversely affects the motor when under high torque.

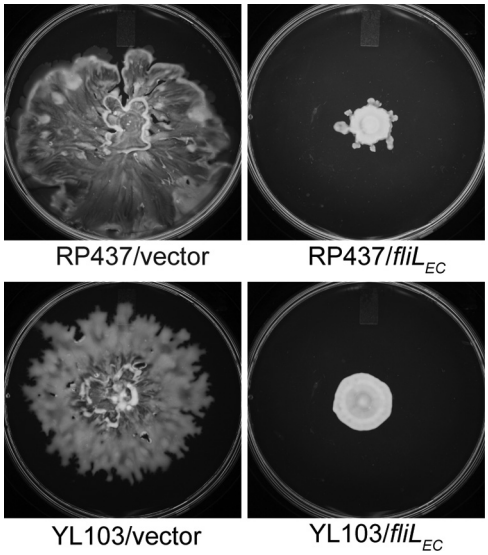

FIG 11 Swarming of wild-type and Δ*fliL* mutant *E. coli* cells in the presence and absence of *E. coli fliL*. Swarming was measured on LB agar containing 0.6% Eiken agar and 0.5% glucose incubated at 30°C for 24 h.

Second, swarming of Δ*fliL* cells is sensitive to temperature and is inhibited at low temperatures. Similar temperature-dependent effects on *P. mirabilis* swarming have been noted by Armbruster et al. (53). The temperature-sensitive motility of Δ*fliL* cells also hints at a role for FliL in modulating motor energetics and suggests that loss of FliL underpowers the motor at low temperatures. At low loads, torque on the motor is exponentially dependent on temperature, while under high-load and high-torque conditions, motor speed is independent of temperature (54, 55). However, under high-load and low-torque conditions, motor speed is temperature dependent (55). When a bacterial cell migrates in a low-viscosity environment, its flagellar motor rotates under low-load conditions. On the other hand, highly viscous environments mimic high-load conditions. As such, the temperature-dependent motility of Δ*fliL* cells hints at a deenergizing of the flagellar motors that presumably produce less power, resulting in a motile force that is insufficient to overcome the physical barriers imposed by the surface.

A substantial body of evidence links the performance of the motor with temperature. For example, point mutations in *S. enterica fliG*, *fliM*, and *fliN*, encoding three proteins of the C-ring flagellar rotor, exhibit a temperature-sensitive (TS) motile phenotype (56). TS mutations have also been found in Na^+-driven motors, and certain mutants with mutations in PomA of *Vibrio alginolyticus*, a MotA stator homologue, also exhibit a TS phenotype (57). Thus, the temperature-dependent phenotype of Δ*fliL* cells offers a clue that suggests FliL interacts with a component of the motor (either stator or rotor) that is involved in torque generation. Moreover, this interaction appears to be torque dependent,

prompting us to speculate that FliL may be acting as a governor to control motor function and/or energetics under high-torque conditions. Although we favor this hypothesis, at present we cannot rule out the possibility that Δ*fliL* cells result in flagellar structural or assembly defects and that it is these defects that result in the temperature-dependent phenotype. Defining the mechanism underlying this FliL temperature-dependent phenotype is an important goal for future research.

With what motor proteins might FliL interact? Several studies have shown structural and functional relationships between FliL, the HBB complex, and the stator. In *P. mirabilis*, mutations not only in *fliL* but also in *fliG* (C-ring) and *fliF* (MS ring) result in the Elo^+ phenotype (8), phenotypically linking FliL, FliG, and FliF and suggesting the three proteins may function in the same "pathway." Fluorescence resonance energy transfer (FRET) data obtained from *E. coli* demonstrate a weak interaction between FliL and FliG (58), cryo-electron tomography images of the flagellar basal body of *B. burgdoferi* have localized FliL adjacent to the stator (29), and genetic data obtained from *R. sphaeroides* (30) and *S. enterica* (59) suggest that FliL interacts with the stator (30, 59, 60).

While evidence of direct interactions between FliL and the stator is lacking, we speculate that FliL enhances the performance of the motor by acting as a molecular governor to limit or control proton flow through the stator when the motor is operating under high-torque conditions, (i.e., in high-viscosity environments), as was recently suggested (61). This hypothesis presumes that under such conditions where flagellar motors are working at peak force, the cell risks acidification of its cytoplasm, which would lead to a potential hyperpolarization of the membrane and death, if left uncontrolled. In this model, FliL interacts with the stator to control the amount of protons flowing through the proton channel of the motor. We hypothesize that in the absence of FliL, unregulated proton flow across the membrane occurs, resulting in deenergizing flagellar motors. One prediction of this hypothesis is that the performance of the Δ*fliL* motor in viscous environments can be improved by increasing energy flow or PMF of the cell, perhaps through efflux of excess H^+ to the external milieu. Investigations testing this hypothesis are under way in our laboratory.

Recent reports have demonstrated that *E. coli* motor stators function as mechanosensors as well as torque-generating units, and the recruitment and assembly of the stator occur in a load-dependent manner (62, 63). This underscores the putative connection between flagellar mechanosensing, FliL, and components of the flagellar motor. Lele, Hosu, and Berg further demonstrated that FliL is not involved in stator recruitment (63). These results do not contradict our findings and emphasize that the function of FliL involves events that occur after the initial stage of motor localization.

While our understanding of the role FliL plays is slowly coming into focus, the function of *fliL* and the protein it encodes remain strangely enigmatic, especially in light of how much is known about the function of bacterial flagellar proteins in general. Two factors appear to complicate our efforts: (i) the function of FliL appears to be at least partially species dependent, as described in the introduction, and (ii) *fliL* defects result in conflicting phenotypes that depend on the how the mutation was constructed. The best examples of this are YL1003 (a group II intron insertion in *fliL*) and YL1006 (Δ*fliL*). The former strain is Swr^-, while YL1006 is Swr^+, the only apparent difference between them being the presence of *fliL* DNA in YL1003. The simplest explanation for this difference is that *fliL* (DNA or mRNA) has a second, regulatory function that controls transcription of *flaA* and other flagellar genes, although how this occurs is currently unknown. Nevertheless, what all *P. mirabilis fliL* mutants have in common is the elongated-cell phenotype (Elo^+) in broth cultures, as well as a loss of the C-terminal domain of the FliL protein, which appears to play an important role in surface sensing (18).

Many studies emphasize a role of the flagellum in mechanosensing of surfaces (2, 8, 64, 65), and the present results demonstrate the importance of FliL in the surface-sensing sensory transduction pathway. To summarize our present results, the data reveal that loss of FliL alters the sensitivity of *P. mirabilis* cells to viscosity by lowering the low-viscosity threshold of the surface-sensing response without affecting the cell's high-viscosity response. Using these results, we have created a working model describing the function of FliL in surface sensing. We hypothesize that FliL functions as a structural component of the flagellum that acts as a governor to control proton flow when the motor is under high-torque conditions. This control is exerted through an interaction between the periplasmic C-terminal domain of FliL and a protein component of the motor, perhaps the plug region of MotB (30). This action is predicted to prevent acidification of the cytoplasm and maintain PMF and cellular energetics under these high-torque conditions. We speculate that a bacterial cell may sense a change in PMF, membrane potential, or a pH gradient when the rotation of its flagella becomes inhibited during contact with a surface. This "surface" signal then initiates swarmer cell differentiation through a pathway that minimally includes UmoA, UmoD, and Rcs proteins and results in increased expression of the flagellar master regulator, $FlhD_4C_2$. It is noteworthy that swarmer cells can be induced in broths by lowering the pH of the medium (66), adding credibility to this prediction.

In conclusion, our study provides a better understanding of bacterial biofilm formation, surface sensing, and the role FliL plays in these process. It also raises several important questions. For example, what protein-protein interactions are important for FliL function, and are these interactions viscosity dependent? How does FliL affect motor function in a temperature-dependent manner? Is PMF, membrane potential, or cytoplasmic pH altered by the Δ*fliL* mutation? What is the molecular signal that a cell responds to upon flagellar mechanosensing? The answers to these questions not only will help us to understand FliL, bacterial swarming, and flagellar motor function, but are likely to provide better insight into the mechanism(s) underlying surface sensing and biofilm formation in other bacterial species. The knowledge gained from answering these questions may be useful in the development of strategies to prevent biofilms and novel therapeutic agents to prevent diseases resulting from bacterial biofilms.

ACKNOWLEDGMENTS

We thank Sandy Parkinson and Rasika Harshey for the gift of *E. coli* strains. We also thank Rayford Payne and Peter Norris for editorial comments and two anonymous reviewers for helpful suggestions.

This work was supported by award MCB-0919820 from the National Science Foundation.

REFERENCES

1. **Monds RD, O'Toole GA.** 2009. The developmental model of microbial biofilms: ten years of a paradigm up for review. Trends Microbiol 17:73–87. http://dx.doi.org/10.1016/j.tim.2008.11.001.

2. **Belas R.** 2013. When the swimming gets tough, the tough form a biofilm. Mol Microbiol **90:**1–5. http://dx.doi.org/10.1111/mmi.12354.
3. **Kearns DB.** 2010. A field guide to bacterial swarming motility. Nat Rev Microbiol **8:**634–644. http://dx.doi.org/10.1038/nrmicro2405.
4. **Mobley HL, Belas R.** 1995. Swarming and pathogenicity of *Proteus mirabilis* in the urinary tract. Trends Microbiol **3:**280–284. http://dx.doi.org/10.1016/S0966-842X(00)88945-3.
5. **Coker C, Poore CA, Li X, Mobley HL.** 2000. Pathogenesis of *Proteus mirabilis* urinary tract infection. Microbes Infect **2:**1497–1505. http://dx.doi.org/10.1016/S1286-4579(00)01304-6.
6. **Jacobsen SM, Stickler DJ, Mobley HL, Shirtliff ME.** 2008. Complicated catheter-associated urinary tract infections due to *Escherichia coli* and *Proteus mirabilis*. Clin Microbiol Rev **21:**26–59. http://dx.doi.org/10.1128/CMR.00019-07.
7. **Alavi M, Belas R.** 2001. Surface sensing, swarmer cell differentiation, and biofilm development. Methods Enzymol **336:**29–40. http://dx.doi.org/10.1016/S0076-6879(01)36575-8.
8. **Belas R, Suvanasuthi R.** 2005. The ability of *Proteus mirabilis* to sense surfaces and regulate virulence gene expression involves FliL, a flagellar basal body protein. J Bacteriol **187:**6789–6803. http://dx.doi.org/10.1128/JB.187.19.6789-6803.2005.
9. **Allison C, Lai HC, Hughes C.** 1992. Co-ordinate expression of virulence genes during swarm-cell differentiation and population migration of *Proteus mirabilis*. Mol Microbiol **6:**1583–1591. http://dx.doi.org/10.1111/j.1365-2958.1992.tb00883.x.
10. **Williams FD, Schwarzhoff RH.** 1978. Nature of the swarming phenomenon in *Proteus*. Annu Rev Microbiol **32:**101–122. http://dx.doi.org/10.1146/annurev.mi.32.100178.000533.
11. **Rauprich O, Matsushita M, Weijer CJ, Siegert F, Esipov SE, Shapiro JA.** 1996. Periodic phenomena in *Proteus mirabilis* swarm colony development. J Bacteriol **178:**6525–6538.
12. **Berg HC.** 2003. The rotary motor of bacterial flagella. Annu Rev Biochem **72:**19–54. http://dx.doi.org/10.1146/annurev.biochem.72.121801.161737.
13. **Chevance FF, Hughes KT.** 2008. Coordinating assembly of a bacterial macromolecular machine. Nat Rev Microbiol **6:**455–465. http://dx.doi.org/10.1038/nrmicro1887.
14. **Liu X, Matsumura P.** 1994. The FlhD/FlhC complex, a transcriptional activator of the *Escherichia coli* flagellar class II operons. J Bacteriol **176:**7345–7351.
15. **Liu X, Matsumura P.** 1996. Differential regulation of multiple overlapping promoters in flagellar class II operons in *Escherichia coli*. Mol Microbiol **21:**613–620. http://dx.doi.org/10.1111/j.1365-2958.1996.tb02569.x.
16. **Furness RB, Fraser GM, Hay NA, Hughes C.** 1997. Negative feedback from a *Proteus* class II flagellum export defect to the *flhDC* master operon controlling cell division and flagellum assembly. J Bacteriol **179:**5585–5588.
17. **Morgenstein RM, Szostek B, Rather PN.** 2010. Regulation of gene expression during swarmer cell differentiation in *Proteus mirabilis*. FEMS Microbiol Rev **34:**753–763. http://dx.doi.org/10.1111/j.1574-6976.2010.00229.x.
18. **Cusick K, Lee YY, Youchak B, Belas R.** 2012. Perturbation of FliL interferes with *Proteus mirabilis* swarmer cell gene expression and differentiation. J Bacteriol **194:**437–447. http://dx.doi.org/10.1128/JB.05998-11.
19. **Pearson MM, Rasko DA, Smith SN, Mobley HL.** 2010. Transcriptome of swarming *Proteus mirabilis*. Infect Immun **78:**2834–2845. http://dx.doi.org/10.1128/IAI.01222-09.
20. **Majdalani N, Gottesman S.** 2005. The Rcs phosphorelay: a complex signal transduction system. Annu Rev Microbiol **59:**379–405. http://dx.doi.org/10.1146/annurev.micro.59.050405.101230.
21. **Francez-Charlot A, Laugel B, Van Gemert A, Dubarry N, Wiorowski F, Castanie-Cornet MP, Gutierrez C, Cam K.** 2004. RcsCDB His-Asp phosphorelay system negatively regulates the *flhDC* operon in *Escherichia coli*. Mol Microbiol **49:**823–832. http://dx.doi.org/10.1046/j.1365-2958.2003.03601.x.
22. **Belas R, Schneider R, Melch M.** 1998. Characterization of *Proteus mirabilis* precocious swarming mutants: identification of *rsbA*, encoding a regulator of swarming behavior. J Bacteriol **180:**6126–6139.
23. **Liaw SJ, Lai HC, Ho SW, Luh KT, Wang WB.** 2001. Characterisation of *p*-nitrophenylglycerol-resistant *Proteus mirabilis* super-swarming mutants. J Med Microbiol **50:**1039–1048.
24. **Clemmer KM, Rather PN.** 2007. Regulation of *flhDC* expression in *Proteus mirabilis*. Res Microbiol **158:**295–302. http://dx.doi.org/10.1016/j.resmic.2006.11.010.
25. **Dufour A, Furness RB, Hughes C.** 1998. Novel genes that upregulate the *Proteus mirabilis flhDC* master operon controlling flagellar biogenesis and swarming. Mol Microbiol **29:**741–751. http://dx.doi.org/10.1046/j.1365-2958.1998.00967.x.
26. **Morgenstein RM, Rather PN.** 2012. Role of the Umo proteins and the Rcs phosphorelay in the swarming motility of the wild type and an O-antigen (*waaL*) mutant of *Proteus mirabilis*. J Bacteriol **194:**669–676. http://dx.doi.org/10.1128/JB.06047-11.
27. **Attmannspacher U, Scharf BE, Harshey RM.** 2008. FliL is essential for swarming: motor rotation in absence of FliL fractures the flagellar rod in swarmer cells of *Salmonella enterica*. Mol Microbiol **68:**328–341. http://dx.doi.org/10.1111/j.1365-2958.2008.06170.x.
28. **Schoenhals GJ, Macnab RM.** 1999. FliL is a membrane-associated component of the flagellar basal body of *Salmonella*. Microbiology **145:**1769–1775. http://dx.doi.org/10.1099/13500872-145-7-1769.
29. **Motaleb MA, Pitzer JE, Sultan SZ, Liu J.** 2011. A novel gene inactivation system reveals altered periplasmic flagellar orientation in a *Borrelia burgdorferi fliL* mutant. J Bacteriol **193:**3324–3331. http://dx.doi.org/10.1128/JB.00202-11.
30. **Suaste-Olmos F, Domenzain C, Mireles-Rodriguez JC, Poggio S, Osorio A, Dreyfus G, Camarena L.** 2010. The flagellar protein FliL is essential for swimming in *Rhodobacter sphaeroides*. J Bacteriol **192:**6230–6239. http://dx.doi.org/10.1128/JB.00655-10.
31. **Jenal U, White J, Shapiro L.** 1994. *Caulobacter* flagellar function, but not assembly, requires FliL, a non-polarly localized membrane protein present in all cell types. J Mol Biol. **243:**227–244. http://dx.doi.org/10.1006/jmbi.1994.1650.
32. **Belas R, Horikawa E, Aizawa S, Suvanasuthi R.** 2009. Genetic determinants of *Silicibacter* sp. TM1040 motility J Bacteriol **191:**4502–4512. http://dx.doi.org/10.1128/JB.00429-09.
33. **Raha M, Sockett H, Macnab RM.** 1994. Characterization of the *fliL* gene in the flagellar regulon of *Escherichia coli* and *Salmonella typhimurium*. J Bacteriol **176:**2308–2311.
34. **Lee YY, Patellis J, Belas R.** 2013. Activity of *Proteus mirabilis* FliL is viscosity dependent and requires extragenic DNA. J Bacteriol **195:**823–832. http://dx.doi.org/10.1128/JB.02024-12.
35. **Belas R, Erskine D, Flaherty D.** 1991. *Proteus mirabilis* mutants defective in swarmer cell differentiation and multicellular behavior. J Bacteriol **173:**6279–6288.
36. **Segura A, Duque E, Hurtado A, Ramos JL.** 2001. Mutations in genes involved in the flagellar export apparatus of the solvent-tolerant *Pseudomonas putida* DOT-T1E strain impair motility and lead to hypersensitivity to toluene shocks. J Bacteriol **183:**4127–4133. http://dx.doi.org/10.1128/JB.183.14.4127-4133.2001.
37. **Belas R, Erskine D, Flaherty D.** 1991. Transposon mutagenesis in *Proteus mirabilis*. J Bacteriol **173:**6289–6293.
38. **Parkinson JS, Houts SE.** 1982. Isolation and behavior of *Escherichia coli* deletion mutants lacking chemotaxis functions. J Bacteriol **151:**106–113.
39. **Kolter R, Inuzuka M, Helinski DR.** 1978. Trans-complementation-dependent replication of a low molecular weight origin fragment from plasmid R6K. Cell **15:**1199–1208. http://dx.doi.org/10.1016/0092-8674(78)90046-6.
40. **Simon R, Priefer U, Puhler A.** 1983. A broad host range mobilization system for *in vivo* genetic engineering: transposon mutagenesis in gram negative bacteria. Nat Biotechnol **1:**784–791. http://dx.doi.org/10.1038/nbt1183-784.
41. **Baba T, Ara T, Hasegawa M, Takai Y, Okumura Y, Baba M, Datsenko KA, Tomita M, Wanner BL, Mori H.** 2006. Construction of *Escherichia coli* K-12 in-frame, single-gene knockout mutants: the Keio collection. Mol Syst Biol. **2:**2006.0008. http://dx.doi.org/10.1038/msb4100050.
42. **Miller VL, Mekalanos JJ.** 1988. A novel suicide vector and its use in construction of insertion mutations: osmoregulation of outer membrane proteins and virulence determinants in *Vibrio cholerae* requires *toxR*. J Bacteriol **170:**2575–2583.
43. **Kaniga K, Delor I, Cornelis GR.** 1991. A wide-host-range suicide vector for improving reverse genetics in gram-negative bacteria: inactivation of the blaA gene of Yersinia enterocolitica. Gene **109:**137–141. http://dx.doi.org/10.1016/0378-1119(91)90599-7.
44. **Datsenko KA, Wanner BL.** 2000. One-step inactivation of chromosomal genes in *Escherichia coli* K-12 using PCR products. Proc Natl Acad Sci U S A **97:**6640–6645. http://dx.doi.org/10.1073/pnas.120163297.

45. **Cherepanov PP, Wackernagel W.** 1995. Gene disruption in *Escherichia coli*: Tc^R and Km^R cassettes with the option of Flp-catalyzed excision of the antibiotic-resistance determinant. Gene **158:**9–14. http://dx.doi.org/10.1016/0378-1119(95)00193-A.
46. **Neumann E, Schaefer-Ridder M, Wang Y, Hofschneider PH.** 1982. Gene transfer into mouse lyoma cells by electroporation in high electric fields. EMBO J **1:**841–845.
47. **Miller JH.** 1992. A short course in bacterial genetics. Cold Spring Harbor Laboratory Press, Cold Spring Harbor, NY.
48. **Lee YY, Barker CS, Matsumura P, Belas R.** 2011. Refining the binding of the *Escherichia coli* flagellar master regulator, $FlhD_4C_2$, on a base-specific level. J Bacteriol **193:**4057–4068. http://dx.doi.org/10.1128/JB.00442-11.
49. **Livak KJ, Schmittgen TD.** 2001. Analysis of relative gene expression data using real-time quantitative PCR and the 2^{-DDCT} method. Methods **25:**402–408. http://dx.doi.org/10.1006/meth.2001.1262.
50. **Be'er A, Harshey RM.** 2011. Collective motion of surfactant-producing bacteria imparts superdiffusivity to their upper surface. Biophys J **101:**1017–1024. http://dx.doi.org/10.1016/j.bpj.2011.07.019.
51. **Partridge JD, Harshey RM.** 2013. Swarming: flexible roaming plans. J Bacteriol **195:**909–918. http://dx.doi.org/10.1128/JB.02063-12.
52. **Hay NA, Tipper DJ, Gygi D, Hughes C.** 1997. A nonswarming mutant of Proteus mirabilis lacks the Lrp global transcriptional regulator. J Bacteriol **179:**4741–4746.
53. **Armbruster CE, Hodges SA, Mobley HL.** 2013. Initiation of swarming motility by Proteus mirabilis occurs in response to specific cues present in urine and requires excess L-glutamine. J Bacteriol **195:**1305–1319. http://dx.doi.org/10.1128/JB.02136-12.
54. **Yuan J, Berg HC.** 2010. Thermal and solvent-isotope effects on the flagellar rotary motor near zero load. Biophys J **98:**2121–2126. http://dx.doi.org/10.1016/j.bpj.2010.01.061.
55. **Chen X, Berg HC.** 2000. Torque-speed relationship of the flagellar rotary motor of Escherichia coli. Biophys J **78:**1036–1041. http://dx.doi.org/10.1016/S0006-3495(00)76662-8.
56. **Mashimo T, Hashimoto M, Yamaguchi S, Aizawa S.** 2007. Temperature-hypersensitive sites of the flagellar switch component FliG in *Salmonella enterica* serovar Typhimurium. J Bacteriol **189:**5153–5160. http://dx.doi.org/10.1128/JB.00061-07.
57. **Fukuoka H, Yakushi T, Homma M.** 2004. Concerted effects of amino acid substitutions in conserved charged residues and other residues in the cytoplasmic domain of PomA, a stator component of Na^+-driven flagella. J Bacteriol **186:**6749–6758. http://dx.doi.org/10.1128/JB.186.20.6749-6758.2004.
58. **Li H, Sourjik V.** 2011. Assembly and stability of flagellar motor in *Escherichia coli*. Mol Microbiol **80:**886–899. http://dx.doi.org/10.1111/j.1365-2958.2011.07557.x.
59. **Partridge JD, Harshey RM.** 2013. More than motility: *Salmonella* flagella contribute to overriding friction and facilitating colony hydration during swarming. J Bacteriol **195:**919–929. http://dx.doi.org/10.1128/JB.02064-12.
60. **Fabela S, Domenzain C, De la Mora J, Osorio A, Ramirez-Cabrera V, Poggio S, Dreyfus G, Camarena L.** 2013. A distant homologue of the FlgT protein interacts with MotB and FliL and is essential for flagellar rotation in *Rhodobacter sphaeroides*. J Bacteriol **195:**5285–5296. http://dx.doi.org/10.1128/JB.00760-13.
61. **Belas R.** 2014. Biofilms, flagella, and mechanosensing of surfaces by bacteria. Trends Microbiol **22:**517–527. http://dx.doi.org/10.1016/j.tim.2014.05.002.
62. **Tipping MJ, Delalez NJ, Lim R, Berry RM, Armitage JP.** 2013. Load-dependent assembly of the bacterial flagellar motor. mBio **4**(4):e00551–13. http://dx.doi.org/10.1128/mBio.00551-13.
63. **Lele PP, Hosu BG, Berg HC.** 2013. Dynamics of mechanosensing in the bacterial flagellar motor. Proc Natl Acad Sci U S A **110:**11839–11844. http://dx.doi.org/10.1073/pnas.1305885110.
64. **Cairns LS, Marlow VL, Bissett E, Ostrowski A, Stanley-Wall NR.** 2013. A mechanical signal transmitted by the flagellum controls signalling in *Bacillus subtilis*. Mol Microbiol **90:**6–21. http://dx.doi.org/10.1111/mmi.12342.
65. **Kawagishi I, Imagawa M, Imae Y, McCarter L, Homma M.** 1996. The sodium-driven polar flagellar motor of marine *Vibrio* as the mechanosensor that regulates lateral flagellar expression. Mol Microbiol **20:**693–699. http://dx.doi.org/10.1111/j.1365-2958.1996.tb02509.x.
66. **Fujihara M, Obara H, Watanabe Y, Ono HK, Sasaki J, Goryo M, Harasawa R.** 2011. Acidic environments induce differentiation of Proteus mirabilis into swarmer morphotypes. Microbiol Immunol **55:**489–493. http://dx.doi.org/10.1111/j.1348-0421.2011.00345.x.

Supplemental Materials

Table S1. Oligonucleotide primers used in this study.

Primer	Sequence (5'→3')[a]	Use
fliLup1480-BamHI_f	ATTGGATCCTACTCAACCTCAGAATACACCC	pYL115 construction
fliMdown1426-XbaI_r	CTGTCTAGAGCGAATACCATATTTATCAG	pYL115 construction
NcoI-fliL154_f	GTCCCATGGTTTACCACGTTTATTCTGCG	pYL117 construction
NcoI-fliLp_r	GAACCATGGCATGGACAGTTAAATTCCTGTTTTG	pYL117 construction
fliLF	GGTGATCGCCATTATTGCAG	YL1006 confirmation
fliL_r	GAGCATCTATCTCTGCCTGTGAAAGG	YL1006 confirmation
fliLpF	GGATCCGTGGTGTCGATATTT	YL1006 confirmation; sequencing
fliLR	AGCGTAACGTGATCCCTATG	YL1006 confirmation; sequencing
EcfliLp-BamHI_f	TGAGGATCCCTTCCCAGCAACAGCAAAG	YL102 and YL103 confirmation; sequencing
EcfliL-HindIII_r	CCAAAGCTTATCGCAGAATAAAAGCGG	YL102 and YL103 confirmation
pKD13-2	TGTAGGCTGGAGCTGCTTCG	YL102 confirmation
flhDp-BamHI_f	GGCGGATCCATTTTAGATTTGTCAATTTTTTATGC	pYL68 construction
flhDp-EcoRI_r	ACTGAATTCCTCTTTACATCCCGTCCG	pYL68 construction
fliAp-BamHI_f	AACGGATCCAAGTACCACAAACTGTTCTG	pYL125 construction
fliAp-EcoRI_r	GACGAATTCCCAGAGGCTATTTTTGTCC	pYL125 construction
motAp-BamHI_f	CTTGGATCCTTCAATGTTTTATAATGCTTACCGC	pYL128 construction
motAp-EcoRI_r	GGAGAATTCGATATATCCTAAGAGTACTAACAC	pYL128 construction
umoAp-BamHI_f	CAAGGATCCAACACCAATAGCCATTGC	pYL73 construction
umoAp-EcoRI_r	GCCGAATTCAAATACTCCTTTTTATTACTATTATGATGC	pYL73 construction
flaApF	GGATCCACTGGTCTCCTTTCT	pYL126 construction
flaA'-'lacZ_f	CTATCTAGTTTTACAACGTCGTGACTGGG	pYL126 construction
flaA'-'lacZ_r	GTAAAACTAGATAGTTGGTATTAATGACTTGTGCC	pYL126 construction
lacZ-HindIII_r	TGATAAGCTTTTATTTTTGACACCAGACCAACTGG	pYL68, pYL73, pYL125, pYL126 and pYL128 construction
umoAF	TCCACCACCACCACACGTAA	qRT-PCR
umoAR	CGCAATCCTTTGCCTGTCCTA	qRT-PCR
umoDF	CAAGAGTGCCGTGTTTTCTATA	qRT-PCR
umoDR	CGATGATATCGCCCGGTTTAA	qRT-PCR
rpoAF	GCGTGTTATAGCCCAGTTGA	qRT-PCR
rpoAR	AGGCTGACGAACATCACGTA	qRT-PCR

[a] = underlined sequence, restriction sites for cloning.

Table S2. Migration of wild-type and Δ*fliL* cells at 25°C.

	Colony Diameter[a]			
	23h		96 h	
	Wild-type	Δ*fliL*	Wild-type	Δ*fliL*
Semisolid agar	48.6±1.0	20.7±0.2	>100.00[c]	>100.00[c]
Soft agar	6.6±0.4[b]	7.1±0.4[b]	33.4±3.2	11.9±0.3[b]
Hard agar	28.2±0.9	6.0±0.0[b]	72.9±3.0	9.0±0.2[b]

a = Colony diameter in mm ± standard deviation is the mean of three independent measurements of the diameter of migrating colonies.

b = non-swarming

c = Migration covered the entire plate.

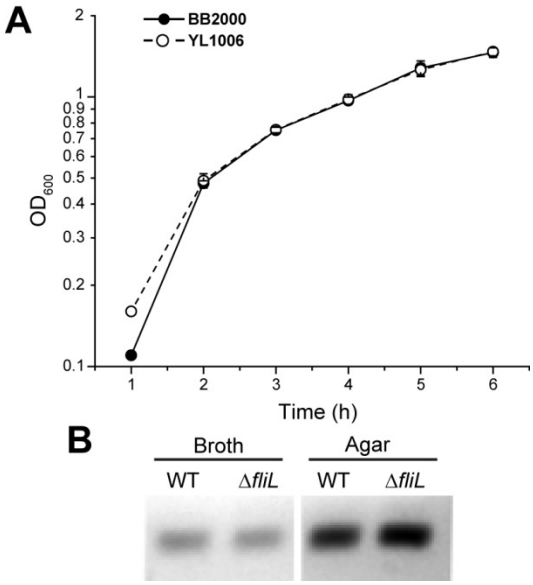

FIG. S1. Deletion of *fliL* does not affect growth and transcription of the downstream gene. (A) Growth curve of the wild-type (BB2000) and Δ*fliL* (YL1006) strains in LB broth. Mean and standard deviation of three independent measurements are shown. (B) RT-PCR transcription of *fliM* in wild-type and Δ*fliL* cells. Thermocycling conditions were as follows: 94°C for 3 min; 30 cycles of 94°C for 1 min, 60°C for 30 s, and 72°C for 20 s; and 72°C for 2 min [as performed in (1)]. *rpoA* gene was used as the reference gene. *rpoA* expression was unchanged in YL1006 compared with the expression in BB2000 (data not shown). Total RNA was extracted from cells grown in LB broth for 2.75 h or on LB agar for 5 h.

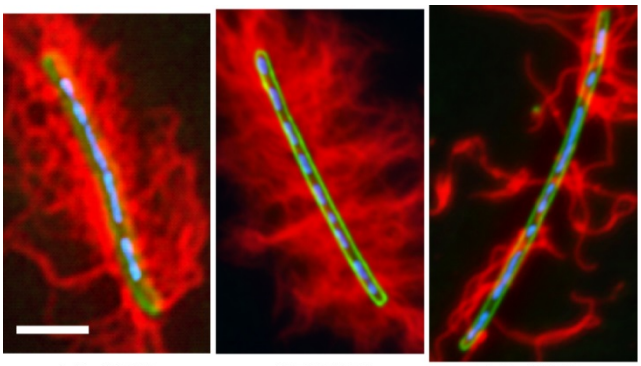

FIG. S2. Morphology of a *P. mirabilis* YL1006 hyperflagellated pseudoswarmer cell (HPC), a YL1003 pseudoswarmer cell (PC) and a wild-type swarmer cell (SC). A representative of each cell type (1000x magnification) with membrane (FM1-43; green), nucleoids (DAPI; blue) and composition with flagellum immunostaining (red). Scale bar: 5 µm.

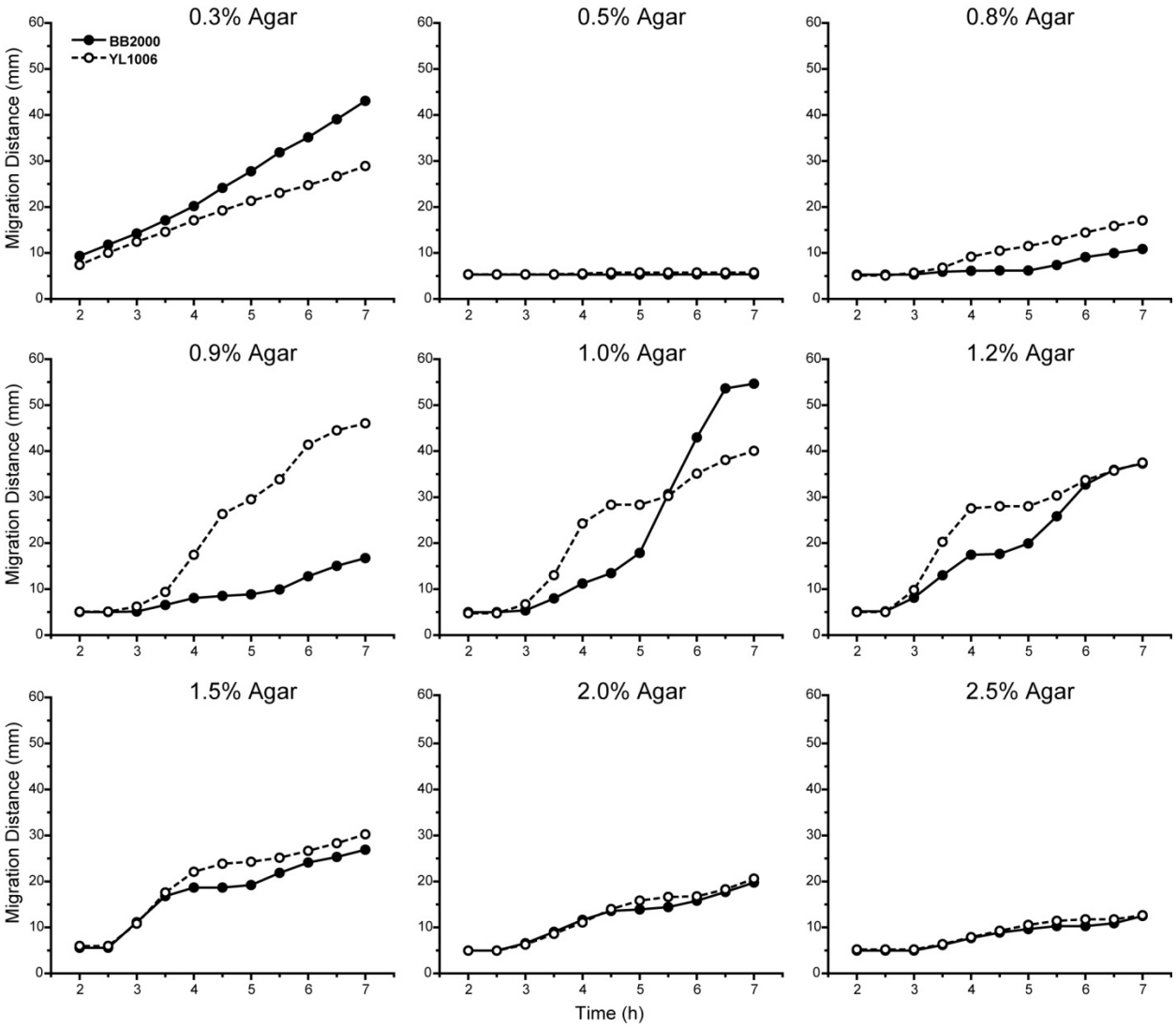

FIG S3. Migration of the wild-type (filled circles) and Δ*fliL* (opened circles) strains on LB with 0.3-2.5% agar.

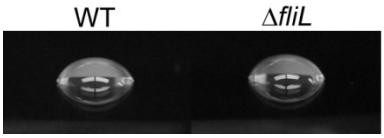

FIG. S4. Drop collapse assay of the supernatant of wild-type and Δ*fliL* cells.

References

1. **Cusick, K., Y. Y. Lee, B. Youchak, and R. Belas.** 2012. Perturbation of FliL interferes with *Proteus mirabilis* swarmer cell gene expression and differentiation. J. Bacteriol. **194:**437-447.